



Published in final edited form as:

*Cogn Affect Behav Neurosci*. 2021 April ; 21(2): 327–346. doi:10.3758/s13415-021-00870-4.

## Overlapping and dissociable brain activations for fluid intelligence and executive functions

**Emiliano Santarnecchi<sup>1</sup>, Davide Momi<sup>1,2</sup>, Lucia Mencarelli<sup>2</sup>, Franziska Plessow<sup>1,3</sup>, Sadhvi Saxena<sup>1</sup>, Simone Rossi<sup>2,4,5</sup>, Alessandro Rossi<sup>2,6</sup>, Santosh Mathan<sup>7</sup>, Alvaro Pascual-Leone<sup>1</sup>**

<sup>1</sup>Berenson-Allen Center for Non-Invasive Brain Stimulation, Beth Israel Deaconess Medical Center, Department of Neurology, Unit of Cognitive Neurology, Harvard Medical School, Boston, MA, USA

<sup>2</sup>Siena Brain Investigation & Neuromodulation Lab (Si-BIN Lab), Department of Medicine, Surgery and Neuroscience, Neurology and Clinical Neurophysiology Section, University of Siena, Siena, Italy

<sup>3</sup>Neuroendocrine Unit, Department of Medicine, Massachusetts General Hospital and Harvard Medical School, Boston, MA, USA

<sup>4</sup>Siena Robotics and Systems Lab (SIRS-Lab), Engineering and Mathematics Department, University of Siena, Siena, Italy

<sup>5</sup>Human Physiology Section, Department of Medicine, Surgery and Neuroscience, University of Siena, Siena, Italy

<sup>6</sup>Medicine, Surgery and Neuroscience Department, University of Siena School of Medicine, Siena, Italy

<sup>7</sup>Honeywell Labs, Honeywell Aerospace, Redmond, WA, USA

### Abstract

Cognitive enhancement interventions aimed at boosting human fluid intelligence (*gf*) have targeted executive functions (EFs), such as updating, inhibition, and switching, in the context of transfer-inducing cognitive training. However, even though the link between EFs and *gf* has been demonstrated at the psychometric level, their neurofunctional overlap has not been quantitatively investigated. Identifying whether and how EFs and *gf* might share neural activation patterns could provide important insights into the overall hierarchical organization of human higher-order cognition, as well as suggest specific targets for interventions aimed at maximizing cognitive transfer. We present the results of a quantitative meta-analysis of the available fMRI and PET literature on EFs and *gf* in humans, showing the similarity between *gf* and (i) the overall global EF network, as well as (ii) specific maps for updating, switching, and inhibition. Results highlight a higher degree of similarity between *gf* and updating (80% overlap) compared with *gf* and

---

Emiliano Santarnecchi, esantarn@bidmc.harvard.edu.

**Supplementary Information** The online version contains supplementary material available at <https://doi.org/10.3758/s13415-021-00870-4>.

Declarations

**Financial disclosures** All authors report no conflict of interest.

inhibition (34%), and *gf* and switching (17%). Moreover, three brain regions activated for both *gf* and each of the three EFs also were identified, located in the left middle frontal gyrus, left inferior parietal lobule, and anterior cingulate cortex. Finally, resting-state functional connectivity analysis on two independent fMRI datasets showed the preferential behavioural correlation and anatomical overlap between updating and *gf*. These findings confirm a close link between *gf* and EFs, with implications for brain stimulation and cognitive training interventions.

## Keywords

Executive functions; Fluid intelligence; fMRI; Functional connectivity; Cognitive enhancement

---

## Introduction

Fluid intelligence (*gf*) has been defined as the ability to cope with novel scenarios irrespective of previously acquired knowledge, identifying and manipulating chunks of available information to drive the emergence of a solution (Cattell, 1987; Cattell, 1963; Horn & Cattell, 1966). Remarkably, *gf* closely correlates with a vast number of cognitive activities and is suggested to be an important predictor of both academic and professional success (Deary et al., 2007; Ren et al., 2015; Rohde & Thompson, 2007; te Nijenhuis et al., 2007; Watkins et al., 2007), as well as overall health and mortality (Gottfredson & Deary, 2004). Given these implications, in the past 20 years a great deal of effort has been devoted to understand the neural correlates underlying *gf* (Ebisch et al., 2012; Jung & Haier, 2007; Prabhakaran et al., 1997). Various theories and models have been proposed (Basten, Hilger, & Fiebach, 2015; Cole, Yarkoni, Repovs, Anticevic, & Braver, 2012; Colom et al., 2009; Ebisch et al., 2012; Langer et al., 2012; Santarnecchi, Rossi, & Rossi, 2015a; Wang, Song, Jiang, Zhang, & Yu, 2011), with a general agreement on the contribution of a bilateral network of brain regions predominantly comprised of the prefrontal and parietal lobes. This has led to the Parieto-Frontal Integration theory of intelligence (P-FIT) (Jung & Haier, 2007), a model describing the most relevant regions involved in intelligence-related processing, as well as their specific role and interplay during cognitive processing. Moreover, a recent meta-analysis supports the frontoparietal network (FPN) as a pivotal component supporting abstract reasoning abilities (Santarnecchi et al., 2017) and also highlights the relevance of a subset of resting-state networks (RSNs) (Sporns, 2014) linked to awareness, salience processing, and attention (Santarnecchi et al., 2017). Moreover, several recent studies highlighted that similarity between task and rest functional connectivity within brain networks is related to behavioral performance (Schultz & Cole, 2016; Zuo et al., 2018).

While a better understanding of neurophysiological underpinnings of *gf* can help to identify neuroanatomic targets for *gf* enhancement, in the past decade a large number of studies have instead focused on developing cognitive training interventions to enhance executive functions (EFs), the complex set of functions that allows for voluntary behavior toward long-term goals. A widely used model of EFs by Miyake et al. (2000) proposes three core competencies that while being correlated show clear distinction between them, namely (i) switching of task or goal sets (“switching”), (ii) updating and monitoring of

working memory representations (“updating”), and (iii) inhibition of prepotent responses (“inhibition”) (Miyake et al., 2000). This concept of “unity and diversity of EFs” has been replicated in many subsequent studies (Fisk & Sharp, 2004; Friedman et al., 2006; Hedden & Yoon, 2006; Huizinga et al., 2006; Lehto et al., 2003; van der Sluis et al., 2007), including neuroimaging ones showing activation of frontoparietal brain regions during EF tasks but also different activation in frontal and/or posterior areas unique to switching and updating (Collette et al., 2005; Sylvester et al., 2003). Of these core EFs, the vast majority of studies has focused on training updating ability (Baltes et al., 1989; Harrison et al., 2013; Jaeggi et al., 2008; Jaeggi et al., 2011) (for a review see: Au et al., 2015) with the goal of inducing a positive transfer to *gf*. This research was guided by a large set of psychometric studies showing a correlation between *gf* and EF abilities (Friedman et al., 2006; McCabe et al., 2010; Miyake et al., 2000; Salthouse et al., 2003; Salthouse & Davis, 2006; Salthouse & Pink, 2008) and lesion studies showing EF and *gf* being both susceptible to frontal lobe lesions (Barbey et al., 2014; Duncan et al., 1995; Roca et al., 2010; Woolgar et al., 2010). In more detail, there are approximately 40 published studies designed to enhance *gf* by means of EF training, most of them based on single (Halford et al., 2007; Jaušovec & Jaušovec, 2012; Studer et al., 2009) or dual-task working-memory trainings tested in adults (Jaeggi et al., 2008; Thompson et al., 2013). In addition, some studies have attempted to enhance *gf* by improving WM in neurotypical children (Zhao et al., 2011) and children with attention-deficit/hyperactivity disorder (Klingberg et al., 2002). While latent factor analysis of behavioral data would suggest high overlap between EFs and *gf*, and therefore the potential for transfer of abilities to *gf*, results have been controversial so far. Some studies reported a benefit (Jaeggi et al., 2008; Jaušovec & Jaušovec, 2012), and others showed no impact of EF training on *gf* (Foroughi et al., 2016; Thompson et al., 2013). In addition, to date, the overlap between *gf* and switching, updating, and inhibition remains purely psychometric; no study investigated the quantitative functional overlap of brain networks across EFs and *gf*. While several studies found a highly correlation between EFs (especially updating) and *gf*, others reported that this could be a methodological error regarding the measurement of the EFs (Frischkorn et al., 2019; Hedge et al., 2018; Rey-Mermet et al., 2019). Looking further, they suggested that the highly correlation between updating and *gf* could be the results of the reliability, characteristic of updating and not of shifting and inhibition. Moreover, these studies point out that updating may be more strongly related to *gf* than any other EFs, because it is not derived as a difference measure. It may simply reflect general WM capacity, while shifting and inhibition may reflect the processing speed (Jewsbury et al., 2016). However, highly correlated behavioral measures may not share the same neural substrates, but only show high levels of covariance, potentially due to the known phenomenon of positive manifold (for a review see: Colom et al., 2016). This term refers to the possibility that different neural regions are the basis of performance on two very different tasks, which, however, are positively related to each other at the behavioral level. This might lead to scenarios where training function “A” might not activate areas relevant for function “B,” therefore leading to no transfer of abilities. At the same time, it might be that increasing one’s ability in function “A” might just be sufficient to increase performance at “B” by making a cognitive subtask linked to “B” -but also relevant for “A” - more efficient. Distinguishing between functional overlap and the phenomenon of positive manifold is not only highly relevant for further advancing the field of cognitive

enhancement but for identifying potential target regions for noninvasive brain stimulation interventions. Thus, characterizing the overlap between the functional networks supporting EF and *gf* represents a critical next step toward improving interventions designed to augment EFs and *gf*. In attempt to quantify the overlap between the functional networks supporting EFs and *gf*, here we present a systematic quantitative meta-analysis of functional magnetic resonance imaging (fMRI) and positron emission tomography (PET) data collected during EFs- and *gf*-related processing. Data were gathered from 163 papers and analyzed within the Activation Likelihood Estimate (ALE) analytic framework (Eickhoff et al., 2009). Separate meta-analytic maps were created for switching, updating, and inhibition, classifying existing literature on the basis of the Miyake's influential EF model (Miyake et al., 2000). As the core of the present investigation, a DICE similarity index was calculated between each EF map and the *gf* meta-analytic map recently published by our group (Santarnecchi et al., 2017). Specific cortical and subcortical overlaps were identified for each pair, allowing us to generate potential hypotheses about switching-, updating-, and inhibition-specific overlaps with *gf*. In addition, regions showing full overlap among all three EFs and *gf* were identified, because they would likely represent the most suitable target for generating EF→*gf* transfer. According to previous behavioral evidence, we predicted a greater degree of overlap for updating and *gf*, with a major contribution by shared regions in the prefrontal and parietal lobes, bilaterally.

Finally, given previous evidence of a specific correlation structure between *gf* and EFs scores in neurotypical individuals (Salthouse et al., 1998; Salthouse et al., 2003), suggesting a stronger link between updating and *gf* and close to no correlation between *gf* and inhibition/switching (Engle et al., 1999; Salthouse & Pink, 2008), we analyzed behavioral data from two independent databases, looking at behavioral correlations across the four cognitive functions. According to prior literature, we hypothesized a stronger similarity/correlation between behavioral data related to *gf* and updating and lower correlations between *gf*, inhibition, and switching.

## Materials and Methods

A quantitative ALE meta-analysis of the available literature about *gf*, inhibition, updating, and switching was performed. A statistical comparison of the resulting maps was performed using the software GingerALE. The similarity between *gf* and EF was tested by analyzing resting-state fMRI data from two datasets collected in Boston (MA, USA) and Siena (Italy). Moreover, a parallel analysis on behavioral data was performed to verify whether observed similarity in connectivity was reflected in the psychometric interaction of EF and *gf* tasks. Details about the analysis are reported below.

### Quantitative meta-analysis comparison

#### Literature search and database creation

**Executive functions:** Potentially relevant articles were retrieved by performing a search in PubMed and Google Scholar databases without temporal restrictions. To specify the object of the present review, terms such as “executive function,” “inhibition,” “updating,” “flexibility,” “switching,” “switching,” “frontal functioning,” and “working memory” were

individually combined with “functional magnetic resonance imaging,” “positron emission tomography,” and related abbreviations (fMRI, PET). The searches for methods and research topics were combined with AND operator. We screened 268 publications from which we excluded 105 using several exclusion criteria: (i) studies including patients with organic illness, (ii) review papers, (iii) studies not reporting fMRI/PET activation coordinates in Montreal Neurologic Institute (MNI) or Talairach space, (iv) studies using a priori-defined regions of interest, and (v) studies not reporting activation foci in table format or reporting statistical values without corresponding coordinates. The final sample was composed by 163 publications (updating = 65; switching = 21; inhibition = 77) (Figure S1). As shown in Table S1, for each study, the following information was retrieved: (i) sample size, (ii) cognitive task, (iii) coordinate system, and (iv) number of foci. Different maps were created, carefully inspecting each manuscript and extracting activation foci from tables referring to the contrast of interest. A list of the publications considered is reported in Table S1.

**Fluid intelligence:** Data from a recently published set of maps by our group were used (Santarnecchi et al., 2017). Specifically, even though the available ALE database includes ten *gf*-related maps (including functional activations, e.g., for verbal and visuospatial material, as well as related to cognitive processing stages, such as Rule Inference and Rule Application), we focused on identifying of a more general overlap between EFs and *gf*. Therefore, we used the general *gf* map (corresponding to the data shown in Fig. 1 and Table 1 in Emiliano Santarnecchi et al., 2017).

**ALE maps computation**—The quantitative evaluation of spatial fMRI patterns was carried out using the activation likelihood estimate (ALE) method implemented in GingerALE software v2.3.2 ([www.brainmap.org](http://www.brainmap.org)) (Eickhoff et al., 2012; Eickhoff et al., 2009). Differently from within-study SPM analysis where every voxel in the image space is tested against a null hypothesis of no activation, the ALE method assumes that for each study of interest there is a given spatial distribution of activity and an associated set of maximal coordinates. Therefore, the algorithm tests to what extent the spatial locations of the activation foci correlate across independently conducted fMRI studies investigating the same construct.

First, the lists of coordinates were carefully checked for duplication of data across publications in order to avoid artefactual inflation of a given foci significance. Coordinates collected from studies reporting activation foci in Talairach space were converted into the MNI space using the tal2mni algorithm implemented in GingerALE. Activation foci from each study were modeled as Gaussian distributions and merged into a single 3D volume. The ALE algorithm modeled spatial uncertainty of each activation focus (Turkeltaub et al., 2012), using an estimation of the intersubject and interstudy variability typically observed in neuroimaging experiments, rather than applying a priori full-width half maximum (FWHM) kernel. Therefore, the number of participants in a given study influenced the spatial extent of the Gaussian function used. We first modeled the probability of activation over all the studies at each spatial point in the brain, returning localized “activation likelihood estimates” or ALE values. Values were then compared with a null distribution created from simulated datasets with randomly placed foci, in order to identify significantly activated clusters

(permutations test = 1,000 run). Following Eickhoff and colleagues arguments supporting a better balance between sensitivity and specificity for Cluster-based corrections over False-Discovery-Rate (FDR) and Family Wise Error (FWE) approaches (Eickhoff, Bzdok, Laird, Kurth, & Fox, 2012), we applied cluster correction for multiple comparisons with a  $p < 0.001$  threshold for cluster-formation and a  $p < 0.05$  for cluster-level inference. Only clusters with a size exceeding the cluster size recommended by ALE were reported (range 500–1,000  $\text{mm}^3$ ).

**Quantitative ALE overlap analysis**—Specific statistical comparisons were computed in order to identify segregated neurobiological signatures of each EFs component as well as conjunction maps showing (i) conjunctions and disjunctions between EFs and *gf* (e.g., updating and *gf*) and (ii) significant overlap between core EFs (e.g., updating and inhibition, see supplementary information). The procedure involved the creation of a combined map, including the two maps of interest (i.e., including all the activation foci), using the voxel-wise minimum value of the input ALE images. Contrast images were created from the subtraction of each pair of ALE maps, together with a map showing their statistically significant overlap. Given that the resulting subtraction image has the major drawback of not considering the differences in the dataset sizes between the two original maps, GingerALE's simulated data of the pooled foci datasets, obtained by randomly dividing the pooled data into two new groupings of the same size as the original datasets. An ALE image was created for each new dataset, subtracted from the other and then compared to the real data. The process was computed 10,000 times, and a voxel-wise  $p$  value image was obtained. Values in each voxel represent the position of real data with respect to the distribution of values obtained during the permutation test. To ease the comprehension of the results, ALE contrast images were converted to Z scores.

This procedure was applied to each of the aforementioned coordinate lists. In particular, we created significant maps showing conjunction and disjunction between updating and *gf*, switching and *gf*, and inhibition and *gf*. Moreover, only the conjunction maps have been created for updating and switching, updating and inhibition, and switching and inhibition (see supplementary information). Results were then expressed as clusters of activation using Z score values in the image statistics and maxima value. Anatomical labels of final cluster locations were provided by the Talairach Daemon (<http://www.talairach.org/daemon.html>). ALE maps were visualized using MriCronGL64 (Rorden & Brett, 2000) on an MNI standard brain.

### Connectivity and behavioral analysis

**fMRI datasets**—In order to test the similarity between *gf* and EFs in terms of connectivity profile, two independent fMRI datasets including resting-state fMRI and cognitive data were used to provide more robust estimates. Data were collected as part of two initiatives respectively looking (i) at the possibility of enhancing *gf* via a combination of cognitive training and non-invasive brain stimulation (i.e., Flexible Adaptive Synergistic Training [FAST], a study funded under the scope of the IARPA SHARP program, collected at the Beth Israel Deaconess Medical Center, Harvard Medical School, Boston, MA; “FAST” dataset hereafter), and (ii) investigating a possible link between spontaneous

fMRI connectivity, cognitive profile, and response to brain stimulation (i.e., the APOLLO study, collected at the University of Siena School of Medicine, Italy; “APOLLO” dataset hereafter). Both initiatives included the acquisition of resting-state fMRI data and behavioral assessments of *gf* and EFs. The **FAST dataset** includes 84 healthy participants (mean age 29 years, range 21–49, standard deviation [SD] = 12; mean education 15 years, range 11–23, SD = 3) with fMRI data and two *gf* measures, namely the Raven Advanced Progressive Matrices (RAPM) (Raven et al., 1998) and the Sandia matrix (Matzen et al., 2010)+. The **APOLLO dataset** includes 130 healthy participants (mean age 25 years, range 19–32, SD = 7; mean education 16 years, range 14–23, SD = 3) with fMRI data and RAPM scores. In **FAST**, the average RAPM accuracy was 0.77 (SD = 0.14), while the Sandia accuracy was 62% (SD = 17). In **APOLLO**, average RAPM accuracy was 54% (SD = 15). To provide estimates of the correlation between connectivity and behavior as test-unspecific as possible, RAPM and Sandia scores were averaged in the FAST dataset. In **FAST**, the average updating accuracy was 68% (SD = 16); the average stop-signal reaction time, a marker of inhibition ability with lower values indicating better inhibition, was 257 ms (SD = 84 ms); the average switch costs, an established indicator of switching ability with lower values indicating better switching, were 71 ms (SD = 37 ms). In **APOLLO**, the average updating accuracy was 70% (SD = 19); the average inhibition reaction time was 235 ms (SD = 63 ms); the average switch costs were 64 ms (SD = 60 ms). Details about the fMRI protocols for the FAST and APOLLO datasets, the *gf* and EF tasks used in both datasets, as well as fMRI preprocessing procedures are included in the supplementary materials.

### **fMRI and behavioral analysis**

**Seed-based analysis:** First, a seed-based connectivity analysis was performed looking at the qualitative similarity of voxel-wise connectivity maps of the *gf* and EFs maps. The average BOLD time course during resting-state was retrieved by averaging the signal from all the voxels included in each EFs and *gf* ALE maps. Subsequently, the signal from each map was correlated with that of the remaining voxels in the rest of the brain, resulting in a 3D volume where each voxel value represents the correlation coefficient between its BOLD activity and that of the seed map of interest. Moreover, we also verified whether EF and *gf* maps display strong connectivity with other resting-state fMRI networks, and if EFs and *gf* maps display a stronger correlation between themselves compared with other resting-state networks (RSNs). To this end, the same seed-based connectivity procedure explained previously was performed by using RSNs maps as seed regions. Specifically, the BOLD activity from 14 RSNs (Shirer et al., 2012) was computed. The connectivity between EFs/*gf* maps and the 14 RSNs was then calculated using a multivariate general linear model (GLM).

**Behavioral analysis:** In an attempt to replicate previous behavioral results, individual *gf* scores were correlated (Pearson correlation coefficient) with updating, inhibition, and switching scores in the two independent datasets.

## Results

### ALE Meta-analysis

The results of the ALE meta-analysis are available for download as a nifti. nii volumetric file at [www.tmslab.org/santalab.php](http://www.tmslab.org/santalab.php). The maps include both network-level volumes representing the entire set of regions activated, e.g., for updating, as well as separate .nii files for each node composing the network. For the sake of synthesis, the lists of regions representing each map are presented in separate paragraphs. Detailed information on the anatomical localization of each significant cluster and the relative statistics are reported in dedicated figures and tables. A more in-depth discussion about the meaning of the patterns identified as well as the role of specific regions is provided in the Discussion section.

### EFs maps

A summary of the anatomical profile of the ALE maps for *gf* and EFs is reported in Fig. 1. Details about each EF map are reported below and are part of the supplementary materials of this meta-analysis.

**Updating**—Map and coordinates for the activation pattern elicited during completion of updating tasks are shown in Figure S2 and Table S2. The map includes ten separate clusters highlighting a bilaterally distributed functional organization mainly involving (left) prefrontal and parietal lobes, with additional contribution from cerebellum, fusiform gyrus and precuneus, and subcortical structures, including lentiform nucleus and insula.

**Inhibition**—Map and coordinates for the inhibition tasks are reported in Figure S3 and Table S3. Consistent with many reports on right hemispheric involvement in inhibition tasks (Garavan et al., 1999), the maps include seven distinct nodes localized mostly in the (right) FPN with further activation of cingulate gyrus, superior temporal lobe, and insula.

**Switching**—Activations during tasks involving switching and their respective sets of coordinates are reported in Figure S4 and Table S4. Qualitatively, seven clusters with a more left lateralized activation seem to be present, mostly related to inferior and middle frontal gyrus activation, as well as activation in the inferior parietal lobule and cingulate gyrus.

**Overlap within EFs**—Activations overlapping between each pair of EFs also were computed, looking at e.g. brain regions activated during both updating and switching processing. Results of each pairwise comparison are displayed in Figures S5, S6, and S7 with details about each activation cluster and corresponding MNI coordinates visible in Tables S5, S6, and S7.

### Conjunction and disjunction between *gf* and updating

The resulting map and coordinates for both conjunction and disjunction patterns of activation between *gf* and updating is reported in Fig. 2A and Table 1. The map of overlap includes 12 separate clusters (i.e., nodes) highlighting a bilaterally distributed functional



organization mainly involving (left) prefrontal and parietal lobes with additional contribution from precuneus and subcortical structures including insula.

Moreover, disjunctive maps of activation show a bilateral frontoparietal activation pattern, which was greater for updating than for *gf*, with additional contribution from cerebellum and subcortical regions, such as insula and claustrum, while 2 separate clusters are clearly visible for *gf* rather than for updating, which include the left inferior frontal gyrus and the right caudate (Fig. 3A; Table 1).

### Conjunction and disjunction between *gf* and switching

Map and coordinates for both conjunction and disjunction pattern of activation between *gf* and switching is reported in Fig. 2A and Table 2. A more left-lateralized pattern of activation is present looking at the conjunctive maps with activation of regions placed mostly in the FPN. For the disjunctive maps, five separate clusters of bilateral frontal, parietal, and occipital regions were present for switching, whereas a single node in the left precentral gyrus characterized the pattern of activity during *gf* tasks (Fig. 3B; Table 2).

### Conjunction and disjunction between *gf* and inhibition

Map and coordinates for both conjunction and disjunction pattern of activation between *gf* and inhibition are reported in Fig. 2A and Table 3. A more left-lateralized activation involving FPN is visible for the overlap map, with further participation of precuneus and insula. Disjunctive maps of activation displayed a more right-lateralized activation for inhibition involving regions of frontal, parietal, and temporal lobes. Conversely, a frontoparietal pattern of activation involving the left hemisphere was found for *gf* tasks (Figure 3C; Table 3).

Volume, coordinates, and corresponding Brodmann area, lobe, hemisphere, and regional labels are reported for each cluster included in the ALE map.

### Full overlap between *gf* and EFs

Map and coordinates for the overlapping activation clusters between *gf* and EFs is reported in Fig. 4. A set of regions in the left hemisphere was identified, with coactivation in the anterior cingulate gyrus (ACC) (MNI = -2, 11, 44), middle frontal gyrus (MFG) (MNI = -50, 13, 22), and inferior parietal lobule (IPL) (MNI = -36, -61, 45).

### Functional connectivity profile and behavioral data

Seed-based analysis of *gf* and EFs maps is displayed in Figs. 5 and 6, showing the similarity between *gf* and EFs connectivity patterns. As previously shown in the case of *gf* (Santarnecchi et al., 2017), EFs maps also show resemblance of frontoparietal “cognitive” networks, such as the dorsal attention network (DAN) (Corbetta & Shulman, 2002) and the frontoparietal network (FPN) (Spreng et al., 2012), and display negative connectivity with medial structures of the default mode network (DMN) (Fox et al., 2005; Fransson, 2005). Less similarity is observed between *gf*/EFs connectivity profile and remaining RSNs related to auditory, visual, motor, and language processing (Fig. 6).

To verify the similarity between functional connectivity patterns (Fig. 5) and behavioral data, the correlation between *gf* and EFs scores was computed for both the FAST and APOLLO datasets. Results are shown in Fig. 7, with a pattern suggesting a stronger similarity (i.e., positive correlation) between *gf* and updating, with weak or null correlation between *gf* and inhibition and switching in both FAST (updating-*gf*,  $r = 0.59$ ,  $p < 0.004$ ; switching-*gf*,  $r = 0.13$ ,  $p < 0.146$ ; inhibition-*gf*,  $r = 0.28$ ,  $p < 0.046$ ) and APOLLO (updating-*gf*,  $r = 0.38$ ,  $p < 0.016$ ; switching-*gf*,  $r = 0.11$ ,  $p < 0.326$ ; inhibition-*gf*,  $r = 0.18$ ,  $p < 0.389$ ) datasets.

## Discussion

We performed a meta-analysis of 163 studies using fMRI or PET while participants completed tasks engaging the three core EFs, i.e. updating, switching and inhibition, and created functional localization maps for each function. Classifying available studies on the basis of EF components (update, inhibition, and switching) allowed us to identify spatially segregated networks of cortical and subcortical regions underlying each core EF and their overlap with brain regions associated with *gf*. The ALE meta-analysis showed greater overlap between *gf* and updating (80%) with less similarity between *gf* and switching (17%) and inhibition (34%). An analysis of behavioral data from two independent datasets also confirmed results of the ALE MRI meta-analysis, as well as previously reported behavioral associations between EFs and *gf*, with an almost exclusive positive correlation between updating and *gf* scores.

### Overlap between updating and *gf*

From a psychometric point of view, previous studies on non-clinical populations have reported evidence of a close correlation between EFs and *gf* (Carpenter et al., 1990; Engle et al., 1999; Miyake et al., 2001; Salthouse et al., 1998; Salthouse et al., 2003). We demonstrate that this overlap is mostly driven by a similarity in fMRI activation patterns observed for *gf* and updating (80% overlap), with significantly smaller similarity for inhibition (34%) and switching (17%).

Our results are consistent with previous behavioral evidence (Friedman et al., 2006; Gray et al., 2003; Salthouse, 2005) in older adults (Salthouse et al., 2003), young adults (Ackerman et al., 2005), and children (Klingberg et al., 2002; Zhao et al., 2011). The relationship between updating (i.e., WM) and *gf* still represents an open debate, with multiple theories explaining their link. One of the main propositions posits a pivotal role of executive control. Engel, Kane, and Conway believe that executive control, WM and *gf* are connected to each other, and the association between WM and *gf* could be the result of the correct use of domain-wide attentional control, consisting of focusing attention on crucial task-relevant information (Engle & Kane, 2004; Kane & Engle, 2002). In essence, the stability of mental representations of task features is supported by the WM system, where such stability also allows for control and manipulation of information, which in turn facilitates reasoning ability (Shipstead et al., 2016).

On the contrary, others have postulated that the crucial cognitive mechanism underlying *gf* and updating lies in storage capacity more than stability of mental representations,

which allows one to actively maintain distinct chunks of information and flexibly construct task-relevant bindings among them (Chuderski et al., 2012). Moreover, further studies have reinforced such a concept by suggesting that storage capacity could depend on the ability to set flexible and temporary bonds between elements and their positions within a certain mental structure (Oberauer et al., 2008; Shipstead et al., 2012; Sternberg, 2008). According to this theory, storage capacity would be the common denominator between WM and *gf* and, subsequently, serve a functional role for the overlapping regions identified in our study (see below).

To examine whether individual differences in EFs are influenced by genetic or environmental influences, Friedman et al. (2008) conducted a multivariate analysis in twins. They used ACE models to analyze similarity and diversity in the genetic substrate supporting the three core EFs (updating, inhibition, and switching), as well as to study whether genetic variance in a general EFs factor “common EF” (representing the aspect of ability that is common across the three different types of EF tasks) reflects variability in intelligence. They found EF correlation to be 99% heritable while diversity was due primarily to substantial genetic influences only in updating (56%) and switching (42%), showing that unity and diversity between EF are genetic. However, this does not mean that EF abilities are immutable, as heritability explains only about half of the variance between tasks. Moreover, the results demonstrated different genetic substrates between “common EF” and intelligence except for some overlap with updating. This confirmed a previous finding by the same group showing significant behavioral correlations between updating and intelligence but no link between the latter and inhibiting or switching (Friedman et al., 2006). It is important to note that the measure of intelligence used was The Wechsler Adult Intelligence Scale III (WAIS-III), which primarily assesses the crystallized component of intelligence, while our research focused on the fluid component of intelligence.

In the past decade, numerous studies have used this overlap to investigate the claim that gains in WM training might transfer to gains in *gf* by means of increased updating capacity (Au et al., 2015). Despite multiple promising studies reporting *gf* enhancement, other attempts at replication failed to show any sign of cognitive transfer (Thompson et al., 2013). The heterogeneity of results across studies, which aimed to create transfer on *gf* by stimulation of EFs, could be attributed to many factors (Rudebeck et al., 2012; Stephenson & Halpern, 2013; Jaeggi et al., 2008; Redick et al., 2013; Thompson et al., 2013). For example, much of the data on how intelligence relates to different EFs comes from studies using standard clinical neuropsychological tests as measures of EF, but these often have poor reliability (Miyake et al., 2000). Shipstead et al. (2012) have proposed a series of methodological weaknesses that could explain this heterogeneity, including inadequate measurement (i.e., using a single task to measure a construct, such as *gf*), conflation of working memory with short-term memory, and inadequate control groups. Moreover, Jaeggi et al. have suggested that variability may depend on how intrinsically motivated the subjects are as well as on personality differences (Jaeggi, Buschkuhl, Shah, & Jonides, 2014), while an old pioneering work has shown that for transfer of learning to be possible one has to apply skills in a variety of different contexts, as the form in which problems are expressed can limit the extent to which well-developed skills can be seen as being relevant and be applied (Simon & Hayes, 1976). Additionally, the contributions of inhibition and switching

may be very important in transfer contexts, whereas updating could be more relevant in a novel domain. The lack of emphasis of these crucial processes may account for some of the limited transfer. Overall, there is not yet a consensus on the relationship between EF and *gf*. It also is important to consider that most psychometrical data regarding the relation between updating and *gf* have been collected via cross-sectional studies (Shipstead et al., 2016) and that well-designed training-related studies might provide causal evidence of such link. The debate about the correlation between EF and *gf* is still ongoing, and recent studies point out the idea that the lack in understanding this correlation could be related in a difference in EFs measurement (while shifting is derived from difference scores, updating and inhibition are calculated as performance in a specific task condition) (Frischkorn et al., 2019; Hedge et al., 2018; Rey-Mermet et al., 2019).

In a nutshell, our findings suggest that the overlap between EFs and *gf* observed in terms of fMRI activation patterns is not mirrored at the behavioral level, with high similarity for *gf* and updating but smaller overlap for switching and inhibition. However, even though a dominant overlap for updating and *gf* has been reported at both behavioural and neural level, the nature of our analysis does not allow to draw a causal link between neuroanatomical and behavioural similarity. Further studies should disentangle this matter.

### Overlapping Core Regions for *gf* and EFs

In our analysis, we identified a set of brain regions that overlap across *gf* and each EFs functions. These regions, mostly related to a left lateralized FPN similar to what described in the P-FIT theory of intelligence (Jung & Haier, 2007), include the left dorsolateral prefrontal cortex (dlPFC; BA9/46), the left inferior parietal lobule (IPL; BA39/40), and left anterior cingulate cortex (ACC; BA8).

The central role of dlPFC both in EFs and intelligence has been amply demonstrated by multiple fMRI studies in healthy subjects and individuals with dlPFC damage (Barbey et al., 2014; Kievit et al., 2014). Spearman (1927) was the first to theorize that dlPFC has a unique functional role leading to a unified neural architecture for higher cognition (Duncan, 2010; Duncan et al., 2000). Subsequent studies support this framework, demonstrating the activation of dlPFC during EF (Duncan & Owen, 2000), general intelligence (Bishop et al., 2008; Duncan et al., 2000; Esposito et al., 1999; Prabhakaran et al., 1997), as well as *gf* tasks (Blair, 2006; Cole et al., 2012, 2015; Woolgar et al., 2010). The dlPFC is particularly involved during updating tasks but is also engaged in manipulation of information (D'Esposito et al., 1998; Haxby et al., 2000; Mencairelli et al., 2019; Smith & Jonides, 1999). Duncan (2005) confirmed the involvement of dlPFC in both updating and inhibition tasks, as well as perceptual tasks. The literature to date support our finding, suggesting left dlPFC as a crucial hub for high-order cognition.

The role of ACC has been also extensively associated with EFs in humans, given its involvement in error monitoring and top-down control over sensory (Crottaz-Herbette & Menon, 2006) and limbic brain regions (Etkin et al., 2006). Moreover, the correlation between these areas and EFs was supported by several studies underscoring the fundamental role of ACC in relating actions to their consequences (Rushworth et al., 2004), learning and predicting action outcomes, providing a control signal to other brain regions (Alexander

& Brown, 2011), as well as in late-stage aspects of response selection (Banich, 2009). These functions are easily associated with core components of brain activity during EF and *gf* tasks (Bush, 2000; Carter et al., 1998, 1999; Crottaz-Herbette and Menon, 2006). Thus, the presence of ACC among the regions showing full overlap across EFs and *gf* is not surprising. Interestingly, other authors also have stressed the potential role of ACC in modulating arousal-related processes (Braver & Barch, 2006), showing ACC as mostly activated during task-initiation cues and error cues, a potential further proof of its role in both control/monitoring of attention.

Finally, different fMRI studies have suggested that both frontal cortex and parietal regions are involved in switching (Braver et al., 2003; Crone et al., 2006; Liston et al., 2006; Sylvester et al., 2003). Several prefrontal regions seem to be involved in cognitive switching, with regional specializations depending upon the specific type of switching required (e.g., Wisconsin Card Sorting Task, attention shift, location rule switch, etc.) (Kim et al., 2012). The inferior parietal lobule (IPL), on the other hand, seems to be crucial in task switching, specifically in transforming stimulus representations into associated response codes (Andersen et al., 1997; Culham & Kanwisher, 2001). IPL is a heterogeneous area responsible for a vast array of cognitive functions, including sensory motor processing (Iacoboni, 2005; Keyser & Gazzola, 2009), executive control (Seeley et al., 2007; Uddin et al., 2011), automatic attentional process (Mark D'Esposito & Grossman, 1996; Nobre et al., 1997), WM maintenance and manipulation (Tsukiura et al., 2001), and WM processing of auditory verbal and nonverbal information tasks (Mencarelli et al., 2019; Yoo et al., 2004).

Left ACC, IPL, and MFG could represent a network of regions at the very core of high-order cognitive functioning in humans. However, focal lesions to areas with high system density and participation coefficient produce more severe and widespread cognitive deficits than focal lesions to areas of high-degree centrality (Warren et al., 2014). Furthermore, lesion-based studies should look into the differential impact of lesions to “overlapping” regions compared with regions mainly related to one specific function.

### **Similarity of behavior-connectivity correlational structures**

Recent studies have shown how resting-state functional connectivity patterns hold predictive value over evoked brain activity (Tavor et al., 2016), suggesting the idea that spontaneous inter-regional coupling “shape” the metabolic changes required for cognitive performance. Moreover, the same principle seems to apply to behavioral performance, with evidence of a link between resting-state fMRI patterns, performance in a specific behavioral task (e.g., *gf* task) and the degree of “shaping” taking place during such task: the more an individual displays high level of performance in a given function, the more his/her functional activation sustaining such function (i.e., an fMRI activation measured in the MRI scanner during a task) is similar to resting-state activity in the MRI scanner. Additionally, Shultz and Cole (2016) showed that subjects with an optimized intrinsic network configuration for domain-general task performance are more efficient in updating functional networks, suggesting that this ability is a hallmark of high intelligence and highlighting that similarity between task and rest functional connectivity within brain networks is related to behavioral performance (Schultz & Cole, 2016; Zuo et al., 2018).

Following this reasoning, one could hypothesize that, given the previously reported positive correlation between updating and *gf* behavioral performance at rest—also confirmed in our two datasets—the patterns of intrinsic fMRI connectivity for *gf* might show more similarity with updating as well, especially compared with that with inhibition of switching. Although our results could not prove this hypothesis, the notion of the positive/negative correlation among EFs and *gf* is of value, e.g., planning noninvasive brain stimulation interventions where stimulation targets should be selected differently, depending on whether it precedes (i.e., it is delivered at rest) or takes place concurrently to cognitive training (i.e., when a stronger specificity of brain activation could be present; see next paragraph). These concepts should be evaluated and discussed in future studies.

### Exploiting the overlap for cognitive enhancement

The present results shed light into the shared neural basis of *gf* and EFs and might inform studies aimed at generating transfer on *gf* by cognitive training programs based on EFs. Specifically, these maps could indicate the best overlapping areas between *gf* and EF, which, if engaged properly, might maximize the chance of cognitive transfer/enhancement in both neurotypical and atypical populations. Alternatively, interventions based on NIBS could be used to engage such regions with high spatial precision, using both magnetic or electrical transcranial stimulation (Filmer, Dux, & Mattingley, 2014; Rossi, Hallett, Rossini, & Pascual-Leone, 2009; Santarnecchi et al., 2015b; Tatti, Rossi, Innocenti, Rossi, & Santarnecchi, 2016). For example, low-voltage electrical stimulation provides an efficient tool to modulate—excite or inhibit—the activity of an entire network with potential for cognitive enhancement (Santarnecchi, Brem, et al., 2015). Previous neuromodulatory studies have reported an enhancement on *gf* (Santarnecchi et al., 2016; Santarnecchi et al., 2013) and working memory (Polanía et al., 2012) following stimulation of a single region in the left prefrontal lobe or a FPN. We have previously reported the effect of 40hz-tACS on the left middle frontal gyrus (MFG) inducing enhancement of *gf* performance (Santarnecchi et al., 2013) but not of spatial working memory abilities (Santarnecchi et al., 2016). Noninvasive brain stimulation could be used both to causally test and validate the maps of EFs-*gf* overlap identified in the present study, as well as to target shared EF-*gf* substrate to maximise the chance for transfer.

### Limitations of the study and future directions

In this study, we created specific meta-analytic maps for updating, inhibit, and switching and compared them with previously published maps for *gf*. However, it must be considered that such maps represent the average activity over multiple tasks addressing the same function (e.g., for updating, we used fMRI data on N-back and AX-CPT). To fully leverage the power of this “functional overlap” approach, future investigations should evaluate the overlap between specific *gf* and EF tasks, especially when selecting the potential target responsible for cognitive transfer. Moreover, it would be interesting to validate these maps with behavioral data. Future investigations should focus on the relationship between EFs/*gf* maps before and after cognitive training, to understand, e.g., whether baseline correlation between EF as well as their overlap with *gf* are predictive of transfer over *gf* abilities.

Unfortunately, measuring EF is a challenging topic because of the difficulty with its definition and measurement (Jurado & Rosselli, 2007). Tasks considered specific in measuring a particular aspect of EF may not be sensitive for defining the entire process, because it often requires other EF and non-EF processes. Current evidence indicates that each EF ability (e.g., updating) can be separate into what is common across the three main EFs, i.e., “unity,” and what is unique to that ability, or “diversity.” This drives what is commonly known as the “impurity task” problem: an EF task is composed of (i) specific aspect of EF targeted by that task (e.g., shifting), (ii) common aspects of EF, and (iii) non-EF aspects of the task (e.g., visual processing), as well as (iv) nonsystematic variance (Snyder et al., 2015). In addition, the low reliability of EF tasks is an important issue because of the poor correlations they have with other measures (Paap & Sawi, 2016). Considering the interpretation by Miyake et al. (2000), complex EF tasks tend to have relatively low internal and/or test–retest reliability, also because subjects adopt different strategies at different times when performing the tasks. The issue of task sensitivity and reliability need to be considered, because they may lead to false negative/positive findings and conclusions, for example that EF is not impaired in a clinical group (Gustavson et al., 2020; Snyder et al., 2015). Given this background, a limitation of our results is that they cannot prove the reliability of EFs measures, but only their generalizability, because the data have been collected at two different sites. Combining multiple EF and *gf* tasks into larger longitudinal studies, further work is needed to understand the associations between these high-order cognitive functions.

Additionally, we collected the fMRI dataset following the recommendations given in past reports (Damoiseaux et al., 2006; Shehzad et al., 2009; Van Dijk et al., 2009). However, as pointed out in a recent study (Laumann et al., 2015), this could be a limitation when we look at resting state functional connectivity individual differences. Moreover, the FD and DVARS thresholds used for motion censoring (0.5) are both quite liberal by current standards, and this could represent a limitation in our study. However, considering that large resting-state networks with known topographies are being extracted and correlated with equally distributed and large networks (*gf*, EF), we do not believe that these thresholds have a significant influence on the results.

## Conclusions

Understanding the shared neural mechanisms underlying *gf* and EFs might help to understand further the structure of high-order cognition and design better cognitive enhancement/rehabilitation approaches. We stress a major overlap between *gf* and updating compared with inhibition and switching, with a strong involvement of regions of the left FPN supporting both EFs and *gf*.

## Supplementary Material

Refer to Web version on PubMed Central for supplementary material.

## Acknowledgments

ES, FP, SM, and APL were supported by the Office of the Director of National Intelligence (ODNI), Intelligence Advanced Research Projects Activity (IARPA), via 2014-13121700007. The views and conclusions contained herein are those of the authors and should not be interpreted as necessarily representing the official policies or endorsements, either expressed or implied, of the ODNI, IARPA, or the U.S. Government. ES and APL are supported by the BROAD Institute at Harvard-MIT (Boston, MA) via 2016P000351. ES and APL are supported by Defense Advanced Research Projects Agency (DARPA) via HR001117S0030. ES is supported by the Beth Israel Deaconess Medical Center (BIDMC) via the Chief Academic Officer (CAO) Award 2017 and the NIH (P01 AG031720-06A1, R01 MH117063-01, R01 AG060981-01). The content of this paper is solely the responsibility of the authors and does not necessarily represent the official views of Harvard University and its affiliated academic health care centers, and the National Institutes of Health.

## References

- Ackerman PL, Beier ME, & Boyle MO (2005). Working Memory and Intelligence: The Same or Different Constructs? *Psychological Bulletin*, 131(1), 30–60. 10.1037/0033-2909.131.1.30 [PubMed: 15631550]
- Alexander WH, & Brown JW (2011). Medial prefrontal cortex as an action-outcome predictor. *Nature Neuroscience*, 14(10), 1338–1344. 10.1038/nn.2921 [PubMed: 21926982]
- Andersen RA, Snyder LH, Bradley DC, & Xing J. (1997). Multimodal representation of space in the posterior parietal cortex and its use in planning movements. *Annual Review of Neuroscience*, 20(1), 303–330.
- Au J, Sheehan E, Tsai N, Duncan GJ, Buschkuhl M, & Jaeggi SM (2015). Improving fluid intelligence with training on working memory: A meta-analysis. *Psychonomic Bulletin & Review*, 22(2), 366–377. 10.3758/s13423-014-0699-x [PubMed: 25102926]
- Baltes PB, Sowarka D, & Kliegl R. (1989). Cognitive training research on fluid intelligence in old age: What can older adults achieve by themselves? *Psychology and Aging*, 4(2), 217–221. 10.1037/0882-7974.4.2.217 [PubMed: 2789749]
- Banich MT (2009). Executive Function: The Search for an Integrated Account. *Current Directions in Psychological Science*, 18(2), 89–94. 10.1111/j.1467-8721.2009.01615.x
- Barbey AK, Colom R, Paul EJ, & Grafman J. (2014). Architecture of fluid intelligence and working memory revealed by lesion mapping. *Brain Structure and Function*, 219(2), 485–494. 10.1007/s00429-013-0512-z [PubMed: 23392844]
- Basten U, Hilger K, & Fiebach CJ (2015). Where smart brains are different: A quantitative meta-analysis of functional and structural brain imaging studies on intelligence. *Intelligence*, 51, 10–27. 10.1016/j.intell.2015.04.009
- Bishop SJ, Fossella J, Croucher CJ, & Duncan J. (2008). COMT val158met Genotype Affects Recruitment of Neural Mechanisms Supporting Fluid Intelligence. *Cerebral Cortex*, 18(9), 2132–2140. 10.1093/cercor/bhm240 [PubMed: 18252743]
- Blair C. (2006). How similar are fluid cognition and general intelligence? A developmental neuroscience perspective on fluid cognition as an aspect of human cognitive ability. *Behavioral and Brain Sciences*, 29(2), 109–125. 10.1017/S0140525X06009034
- Braver Todd S, Reynolds JR, & Donaldson DI (2003). Neural Mechanisms of Transient and Sustained Cognitive Control during Task Switching. *Neuron*, 39(4), 713–726. 10.1016/S0896-6273(03)00466-5 [PubMed: 12925284]
- Braver TS, & Barch DM (2006). Extracting core components of cognitive control. *Trends Cogn Sci*, 10(12), 529–532. 10.1016/j.tics.2006.10.006 [PubMed: 17071129]
- Bush G. (2000). Cognitive and emotional influences in anterior cingulate cortex. 4(6):215–222. <https://www.ncbi.nlm.nih.gov/pubmed/10827444>
- Carpenter PA, Just MA, & Shell P. (1990). What one intelligence test measures: A theoretical account of the processing in the Raven Progressive Matrices Test. *Psychological Review*, 97(3), 404. [PubMed: 2381998]
- Carter CS, Botvinick MM, & Cohen JD (1999). The contribution of the anterior cingulate cortex to executive processes in cognition. *Rev. Neurosci*, 10(1), 49–57. [PubMed: 10356991]



- Carter CS, Braver TS, Barch DM, Botvinick MM, Noll D, & Cohen JD (1998). Anterior cingulate cortex, error detection, and the online monitoring of performance. *Science*, 280(5364), 747–749. [PubMed: 9563953]
- Cattell RB (1987). *Intelligence: Its Structure, Growth and Action*. Elsevier.
- Cattell Raymond B. (1963). Theory of fluid and crystallized intelligence: A critical experiment. *Journal of Educational Psychology*, 54(1), 1–22.
- Chuderski A, Taraday M, N cka E, & Smole T. (2012). Storage capacity explains fluid intelligence but executive control does not. *Intelligence*, 40(3), 278–295. 10.1016/j.intell.2012.02.010
- Cole MW, Ito T, & Braver TS (2015). Lateral Prefrontal Cortex Contributes to Fluid Intelligence Through Multinetwork Connectivity. *Brain Connectivity*, 5(8), 497–504. 10.1089/brain.2015.0357 [PubMed: 26165732]
- Cole MW, Yarkoni T, Repovs G, Anticevic A, & Braver TS (2012). Global connectivity of prefrontal cortex predicts cognitive control and intelligence. *The Journal of Neuroscience: The Official Journal of the Society for Neuroscience*, 32(26), 8988–8999. 10.1523/JNEUROSCI.0536-12.2012 [PubMed: 22745498]
- Collette F, Van der Linden M, Laureys S, Delfiore G, Degueldre C, Luxen A, & Salmon E. (2005). Exploring the unity and diversity of the neural substrates of executive functioning. *Human Brain Mapping*, 25(4), 409–423. 10.1002/hbm.20118 [PubMed: 15852470]
- Colom R, Chuderski A, & Santarnecci E. (2016). Bridge Over Troubled Water: Commenting on Kovacs and Conway’s Process Overlap Theory. *Psychological Inquiry*, 27(3), 181–189. 10.1080/1047840X.2016.1181513
- Colom R, Haier RJ, Head K, Álvarez-Linera J, Quiroga MÁ, Shih PC, & Jung RE (2009). Gray matter correlates of fluid, crystallized, and spatial intelligence: Testing the P-FIT model. *Intelligence*, 37(2), 124–135. 10.1016/j.intell.2008.07.007
- Corbetta M, & Shulman GL (2002). Control of goal-directed and stimulus-driven attention in the brain. *Nature Reviews Neuroscience*, 3(3), 201–215. 10.1038/nrn755 [PubMed: 11994752]
- Crone EA, Wendelken C, Donohue SE, & Bunge SA (2006). Neural Evidence for Dissociable Components of Task-switching. *Cerebral Cortex*, 16(4), 475–486. 10.1093/cercor/bhi127 [PubMed: 16000652]
- Crottaz-Herbette S, & Menon V. (2006). Where and when the anterior cingulate cortex modulates attentional response: Combined fMRI and ERP evidence. *J Cogn Neurosci*, 18(5), 766–780. 10.1162/jocn.2006.18.5.766 [PubMed: 16768376]
- Culham JC, & Kanwisher NG (2001). Neuroimaging of cognitive functions in human parietal cortex. *Current Opinion in Neurobiology*, 11(2), 157–163. 10.1016/S0959-4388(00)00191-4 [PubMed: 11301234]
- Damoiseaux JS, Rombouts SARB, Barkhof F, Scheltens P, Stam CJ, Smith SM, & Beckmann CF (2006). Consistent resting-state networks across healthy subjects. *Proceedings of the National Academy of Sciences*, 103(37), 13848–13853. 10.1073/pnas.0601417103
- Deary IJ, Strand S, Smith P, & Fernandes C. (2007). Intelligence and educational achievement. *Intelligence*, 35(1), 13–21. 10.1016/j.intell.2006.02.001
- D’Esposito M, Aguirre GK, Zarahn E, Ballard D, Shin RK, & Lease J. (1998). Functional MRI studies of spatial and nonspatial working memory. *Brain Research. Cognitive Brain Research*, 7(1), 1–13. [PubMed: 9714705]
- D’Esposito Mark, & Grossman M. (1996). The Physiological Basis of Executive Function and Working Memory. *The Neuroscientist*, 2(6), 345–352. 10.1177/107385849600200612
- Duncan J. (2005). Frontal lobe function and general intelligence: Why it matters. *Cortex*, 41(2), 215–217. [PubMed: 15714904]
- Duncan J. (2010). The multiple-demand (MD) system of the primate brain: Mental programs for intelligent behaviour. *Trends in Cognitive Sciences*, 14(4), 172–179. 10.1016/j.tics.2010.01.004 [PubMed: 20171926]
- Duncan J, Burgess P, & Emslie H. (1995). Fluid intelligence after frontal lobe lesions. *Neuropsychologia*, 33(3), 261–268. 10.1016/0028-3932(94)00124-8 [PubMed: 7791994]

- Duncan J, & Owen AM (2000). Common regions of the human frontal lobe recruited by diverse cognitive demands. *Trends in Neurosciences*, 23(10), 475–483. 10.1016/S0166-2236(00)01633-7 [PubMed: 11006464]
- Duncan J, Seitz RJ, Kolodny J, Bor D, Herzog H, Ahmed A, Newell FN, & Emslie H. (2000). A Neural Basis for General Intelligence. *Science*, 289(5478), 457–460. 10.1126/science.289.5478.457 [PubMed: 10903207]
- Ebisch SJ, Perrucci MG, Mercuri P, Romanelli R, Mantini D, Romani GL, Colom R, & Saggino A. (2012). Common and unique neuro-functional basis of induction, visualization, and spatial relationships as cognitive components of fluid intelligence. *NeuroImage*, 62(1), 331–342. 10.1016/j.neuroimage.2012.04.053 [PubMed: 22565203]
- Eickhoff SB, Bzdok D, Laird AR, Kurth F, & Fox PT (2012). Activation likelihood estimation meta-analysis revisited. *Neuroimage.*, 59(1095–9572 (Electronic)), 2349–2361. 10.1016/j.neuroimage.2011.09.017
- Eickhoff Simon B., Laird AR, Grefkes C, Wang LE, Zilles K, & Fox PT (2009). Coordinate-based activation likelihood estimation meta-analysis of neuroimaging data: A random-effects approach based on empirical estimates of spatial uncertainty. *Human Brain Mapping*, 30(9), 2907–2926. 10.1002/hbm.20718 [PubMed: 19172646]
- Engle RW, & Kane MJ (2004). Executive attention, working memory capacity, and a two-factor theory of cognitive control. *Psychology of Learning and Motivation*, 44, 145–200.
- Engle RW, Laughlin JE, Stephen W, & Conway AR (1999). Working Memory, short-term memory, and general fluid intelligence: A latent-variable approach. *Journal of Experimental Psychology: General*, 128(3), 309–331. [PubMed: 10513398]
- Eposito G, Kirkby BS, Horn V, D J, Ellmore TM, & Berman KF (1999). Context-dependent, neural system-specific neurophysiological concomitants of ageing: Mapping PET correlates during cognitive activation. *Brain*, 122(5), 963–979. 10.1093/brain/122.5.963 [PubMed: 10355679]
- Etkin A, Egner T, Peraza DM, Kandel ER, & Hirsch J. (2006). Resolving emotional conflict: A role for the rostral anterior cingulate cortex in modulating activity in the amygdala. *Neuron*, 51(6), 871–882. 10.1016/j.neuron.2006.07.029 [PubMed: 16982430]
- Filmer HL, Dux PE, & Mattingley JB (2014). Applications of transcranial direct current stimulation for understanding brain function. *Trends in Neurosciences*, 37(12), 742–753. 10.1016/j.tins.2014.08.003 [PubMed: 25189102]
- Fisk JE, & Sharp CA (2004). Age-related impairment in executive functioning: Updating, inhibition, shifting, and access. *Journal of Clinical and Experimental Neuropsychology*, 26(7), 874–890. 10.1080/13803390490510680 [PubMed: 15742539]
- Foroughi CK, Monfort SS, Paczynski M, McKnight PE, & Greenwood PM (2016). Placebo effects in cognitive training. *Proceedings of the National Academy of Sciences of the United States of America*, 113(27), 7470–7474. 10.1073/pnas.1601243113 [PubMed: 27325761]
- Fox MD, Snyder AZ, Vincent JL, Corbetta M, Essen DCV, & Raichle ME (2005). The human brain is intrinsically organized into dynamic, anticorrelated functional networks. *Proceedings of the National Academy of Sciences*, 102(27), 9673–9678. 10.1073/pnas.0504136102
- Fransson P. (2005). Spontaneous low-frequency BOLD signal fluctuations: An fMRI investigation of the resting-state default mode of brain function hypothesis. *Human Brain Mapping*, 26(1), 15–29. 10.1002/hbm.20113 [PubMed: 15852468]
- Friedman NP, Miyake A, Corley RP, Young SE, DeFries JC, & Hewitt JK (2006). Not All Executive Functions Are Related to Intelligence. *Psychological Science*, 17(2), 172–179. [PubMed: 16466426]
- Friedman NP, Miyake A, Young SE, DeFries JC, Corley RP, & Hewitt JK (2008). Individual differences in executive functions are almost entirely genetic in origin. *Journal of Experimental Psychology: General*, 137(2), 201–225. 10.1037/0096-3445.137.2.201 [PubMed: 18473654]
- Frischkorn GT, Schubert A-L, & Hagemann D. (2019). Processing speed, working memory, and executive functions: Independent or inter-related predictors of general intelligence. *Intelligence*, 75, 95–110. 10.1016/j.intell.2019.05.003

- Garavan H, Ross TJ, & Stein EA (1999). Right hemispheric dominance of inhibitory control: An event-related functional MRI study. *Proceedings of the National Academy of Sciences*, 96(14), 8301–8306. 10.1073/pnas.96.14.8301
- Gottfredson LS, & Deary IJ (2004). Intelligence Predicts Health and Longevity, but Why? *Current Directions in Psychological Science*, 13(1), 1–4. 10.1111/j.0963-7214.2004.01301001.x
- Gray JR, Chabris CF, & Braver TS (2003). Neural mechanisms of general fluid intelligence. *Nature Neuroscience*, 6(3), 316–322. 10.1038/nn1014 [PubMed: 12592404]
- Gustavson DE, Lurquin JH, Michaelson LE, Barker JE, Carruth NP, von Bastian CC, & Miyake A. (2020). Lower general executive function is primarily associated with trait worry: A latent variable analysis of negative thought/affect measures. *Emotion*, 20(4), 557–571. 10.1037/emo0000584 [PubMed: 30816740]
- Halford GS, Cowan N, & Andrews G. (2007). Separating Cognitive Capacity from Knowledge: A New Hypothesis. *Trends in Cognitive Sciences*, 11(6), 236–242. 10.1016/j.tics.2007.04.001 [PubMed: 17475538]
- Harrison TL, Shipstead Z, Hicks KL, Hambrick DZ, Redick TS, & Engle RW (2013). Working Memory Training May Increase Working Memory Capacity but Not Fluid Intelligence. *Psychological Science*, 24(12), 2409–2419. 10.1177/0956797613492984 [PubMed: 24091548]
- Haxby JV, Petit L, Ungerleider LG, & Courtney SM (2000). Distinguishing the functional roles of multiple regions in distributed neural systems for visual working memory. *NeuroImage*, 11(2), 145–156. 10.1006/nimg.1999.0527 [PubMed: 10679186]
- Hedden T, & Yoon C. (2006). Individual differences in executive processing predict susceptibility to interference in verbal working memory. *Neuropsychology*, 20(5), 511–528. 10.1037/0894-4105.20.5.511 [PubMed: 16938014]
- Hedge C, Powell G, & Sumner P. (2018). The reliability paradox: Why robust cognitive tasks do not produce reliable individual differences. *Behavior Research Methods*, 50(3), 1166–1186. 10.3758/s13428-017-0935-1 [PubMed: 28726177]
- Horn JL, & Cattell RB (1966). Refinement and test of the theory of fluid and crystallized general intelligences. *Journal of Educational Psychology*, 57(5), 253–270. [PubMed: 5918295]
- Huizinga M, Dolan CV, & van der Molen MW (2006). Age-related change in executive function: Developmental trends and a latent variable analysis. *Neuropsychologia*, 44(11), 2017–2036. 10.1016/j.neuropsychologia.2006.01.010 [PubMed: 16527316]
- Iacoboni M. (2005). Neural mechanisms of imitation. *Current Opinion in Neurobiology*, 15(6), 632–637. 10.1016/j.conb.2005.10.010 [PubMed: 16271461]
- Jaeggi SM, Buschkuhl M, Jonides J, & Perrig WJ (2008). Improving fluid intelligence with training on working memory. *Proc.Natl.Acad.Sci.U.S.A.*, 105(1091–6490 (Electronic)), 6829–6833. 10.1073/pnas.0801268105 [PubMed: 18198274]
- Jaeggi SM, Buschkuhl M, Jonides J, & Shah P. (2011). Short- and long-term benefits of cognitive training. *Proceedings of the National Academy of Sciences*, 108(25), 10081–10086. 10.1073/pnas.1103228108
- Jaeggi SM, Buschkuhl M, Shah P, & Jonides J. (2014). The role of individual differences in cognitive training and transfer. *Memory & Cognition*, 42(3), 464–480. 10.3758/s13421-013-0364-z [PubMed: 24081919]
- Jaušovec N, & Jaušovec K. (2012). Working memory training: Improving intelligence—changing brain activity. *Brain and Cognition*, 79(2), 96–106. 10.1016/j.bandc.2012.02.007 [PubMed: 22475577]
- Jewsbury PA, Bowden SC, & Strauss ME (2016). Integrating the switching, inhibition, and updating model of executive function with the Cattell-Horn-Carroll model. *Journal of Experimental Psychology. General*, 145(2), 220–245. 10.1037/xge0000119 [PubMed: 26569128]
- Jung RE, & Haier RJ (2007). The Parieto-Frontal Integration Theory (P-FIT) of intelligence: Converging neuroimaging evidence. *Behavioral and Brain Sciences*, 30(02), 135. 10.1017/S0140525X07001185
- Jurado MB, & Rosselli M. (2007). The Elusive Nature of Executive Functions: A Review of our Current Understanding. *Neuropsychology Review*, 17(3), 213–233. 10.1007/s11065-007-9040-z [PubMed: 17786559]

- Kane MJ, & Engle RW (2002). The role of prefrontal cortex in working-memory capacity, executive attention, and general fluid intelligence: An individual-differences perspective. *Psychonomic Bulletin & Review*, 9(4), 637–671. [PubMed: 12613671]
- Keysers C, & Gazzola V. (2009). Expanding the mirror: Vicarious activity for actions, emotions, and sensations. *Current Opinion in Neurobiology*, 19(6), 666–671. 10.1016/j.conb.2009.10.006 [PubMed: 19880311]
- Kievit RA, Davis SW, Mitchell DJ, Taylor JR, Duncan J, Henson RNA, & Cam-CAN Research Team (2014). Distinct aspects of frontal lobe structure mediate age-related differences in fluid intelligence and multitasking. *Nature Communications*, 5, 5658. 10.1038/ncomms6658
- Kim C, Cilles SE, Johnson NF, & Gold BT (2012). Domain General and Domain Preferential Brain Regions Associated with Different Types of Task Switching: A Meta-Analysis. *Human Brain Mapping*, 33(1), 130–142. 10.1002/hbm.21199 [PubMed: 21391260]
- Klingberg T, Forssberg H, & Westerberg H. (2002). Training of Working Memory in Children With ADHD. *Journal of Clinical and Experimental Neuropsychology (Neuropsychology, Development and Cognition: Section A)*, 24(6), 781–791. 10.1076/jcen.24.6.781.8395
- Langer N, Pedroni A, Gianotti LRR, Hänggi J, Knoch D, & Jäncke L. (2012). Functional brain network efficiency predicts intelligence. *Human Brain Mapping*, 33(6), 1393–1406. 10.1002/hbm.21297 [PubMed: 21557387]
- Laumann TO, Gordon EM, Adeyemo B, Snyder AZ, Joo SJ, Chen M-Y, Gilmore AW, McDermott KB, Nelson SM, Dosenbach NUF, Schlaggar BL, Mumford JA, Poldrack RA, & Petersen SE (2015). Functional System and Areal Organization of a Highly Sampled Individual Human Brain. *Neuron*, 87(3), 657–670. 10.1016/j.neuron.2015.06.037 [PubMed: 26212711]
- Lehto JE, Juujärvi P, Kooistra L, & Pulkkinen L. (2003). Dimensions of executive functioning: Evidence from children. *British Journal of Developmental Psychology*, 21(1), 59–80. 10.1348/026151003321164627
- Liston C, Matalon S, Hare TA, Davidson MC, & Casey BJ (2006). Anterior Cingulate and Posterior Parietal Cortices Are Sensitive to Dissociable Forms of Conflict in a Task-Switching Paradigm. *Neuron*, 50(4), 643–653. 10.1016/j.neuron.2006.04.015 [PubMed: 16701213]
- Matzen LE, Benz ZO, Dixon KR, Posey J, Kroger JK, & Speed AE (2010). Recreating Raven's: Software for systematically generating large numbers of Raven-like matrix problems with normed properties. *Behav.Res.Methods*, 42( 1554–3528 (Electronic)), 525–541. 10.3758/BRM.42.2.525
- McCabe DP, Roediger HL, McDaniel MA, Balota DA, & Hambrick DZ (2010). The Relationship Between Working Memory Capacity and Executive Functioning: Evidence for a Common Executive Attention Construct. *Neuropsychology*, 24(2), 222–243. 10.1037/a0017619 [PubMed: 20230116]
- Mencarelli M, Neri N, Davide Momi, Arianna M, Simone R, Alessandro R, & Emiliano S. (2019). Stimuli, presentation modality, and load-specific brain activity patterns during n-back task. *Human Brain Mapping*, hbm.24633. 10.1002/hbm.24633s
- Miyake A, Friedman NP, Emerson MJ, Witzki AH, Howerter A, & Wager TD (2000). The Unity and Diversity of Executive Functions and Their Contributions to Complex “Frontal Lobe” Tasks: A Latent Variable Analysis. *Cognitive Psychology*, 41(1), 49–100. 10.1006/cogp.1999.0734 [PubMed: 10945922]
- Miyake A, Friedman NP, Rettinger DA, Shah P, & Hegarty M. (2001). How are visuospatial working memory, executive functioning, and spatial abilities related? A latent-variable analysis. *Journal of Experimental Psychology: General*, 130(4), 621–640. 10.1037//0096-3445.130.4.621 [PubMed: 11757872]
- Nobre AC, Sebestyen GN, Gitelman DR, Mesulam MM, Frackowiak RS, & Frith CD (1997). Functional localization of the system for visuospatial attention using positron emission tomography. *Brain*, 120(3), 515–533. 10.1093/brain/120.3.515 [PubMed: 9126062]
- Oberauer K, Süß H-M, Wilhelm O, & Sander N. (2008). Individual Differences in Working Memory Capacity and Reasoning Ability. In Conway A, Jarrold C, Kane M, Miyake A, & Towse J. (Eds.), *Variation in Working Memory* (pp. 49–75). Oxford University Press. 10.1093/acprof:oso/9780195168648.003.0003

- Paap KR, & Sawi O. (2016). The role of test-retest reliability in measuring individual and group differences in executive functioning. *Journal of Neuroscience Methods*, 274, 81–93. 10.1016/j.jneumeth.2016.10.002 [PubMed: 27720867]
- Polanía R, Nitsche MA, Korman C, Batsikadze G, & Paulus W. (2012). The Importance of Timing in Segregated Theta Phase-Coupling for Cognitive Performance. *Current Biology*, 22(14), 1314–1318. 10.1016/j.cub.2012.05.021 [PubMed: 22683259]
- Prabhakaran V, Smith JAL, Desmond JE, Glover GH, & Gabrieli JDE (1997). Neural Substrates of Fluid Reasoning: An fMRI Study of Neocortical Activation during Performance of the Raven's Progressive Matrices Test. *Cognitive Psychology*, 33(1), 43–63. 10.1006/cogp.1997.0659 [PubMed: 9212721]
- Raven J, Raven JC, & Court JH (1998). *Manual for Raven's progressive matrices and vocabulary scales*.
- Redick TS, Shipstead Z, Harrison TL, Hicks KL, Fried DE, Hambrick DZ, Kane MJ, & Engle RW (2013). No evidence of intelligence improvement after working memory training: A randomized, placebo-controlled study. *Journal of Experimental Psychology: General*, 142(2), 359–379. 10.1037/a0029082 [PubMed: 22708717]
- Ren X, Schweizer K, Wang T, & Xu F. (2015). The Prediction of Students' Academic Performance With Fluid Intelligence in Giving Special Consideration of Learning. *Advances in Cognitive Psychology*, 11(3), 97–105. 10.5709/acp-0175-z [PubMed: 26435760]
- Rey-Mermet A, Gade M, Souza AS, von Bastian CC, & Oberauer K. (2019). Is executive control related to working memory capacity and fluid intelligence? *Journal of Experimental Psychology: General*, 148(8), 1335–1372. 10.1037/xge0000593 [PubMed: 30958017]
- Roca M, Parr A, Thompson R, Woolgar A, Torralva T, Antoun N, Manes F, & Duncan J. (2010). Executive function and fluid intelligence after frontal lobe lesions. *Brain: A Journal of Neurology*, 133(Pt 1), 234–247. 10.1093/brain/awp269 [PubMed: 19903732]
- Rohde TE, & Thompson LA (2007). Predicting academic achievement with cognitive ability. *Intelligence*, 35(1), 83–92. 10.1016/j.intell.2006.05.004
- Rorden C, & Brett M. (2000). Stereotaxic display of brain lesions. *Behav. Neurol*, 12(4), 191–200. [PubMed: 11568431]
- Rossi S, Hallett M, Rossini PM, & Pascual-Leone A. (2009). Safety, ethical considerations, and application guidelines for the use of transcranial magnetic stimulation in clinical practice and research. *Clinical Neurophysiology*, 120(12), 2008–2039. 10.1016/j.clinph.2009.08.016 [PubMed: 19833552]
- Rudebeck SR, Bor D, Ormond A, O'Reilly JX, & Lee ACH (2012). A Potential Spatial Working Memory Training Task to Improve Both Episodic Memory and Fluid Intelligence. *PLOS ONE*, 7(11), e50431. 10.1371/journal.pone.0050431
- Rushworth MFS, Walton ME, Kennerley SW, & Bannerman DM (2004). Action sets and decisions in the medial frontal cortex. *Trends in Cognitive Sciences*, 8(9), 410–417. 10.1016/j.tics.2004.07.009 [PubMed: 15350242]
- Salthouse TA, Fristoe N, McGuthry KE, & Hambrick DZ (1998). Relation of task switching to speed, age, and fluid intelligence. *Psychology and Aging*, 13(3), 445–461. [PubMed: 9793120]
- Salthouse Timothy A. (2005). Relations Between Cognitive Abilities and Measures of Executive Functioning. *Neuropsychology*, 19(4), 532–545. 10.1037/0894-4105.19.4.532 [PubMed: 16060828]
- Salthouse Timothy A., Atkinson TM, & Berish DE (2003). Executive functioning as a potential mediator of age-related cognitive decline in normal adults. *Journal of Experimental Psychology: General*, 132(4), 566–594. 10.1037/0096-3445.132.4.566 [PubMed: 14640849]
- Salthouse Timothy A., & Davis HP (2006). Organization of cognitive abilities and neuropsychological variables across the lifespan. *Developmental Review*, 26(1), 31–54. 10.1016/j.dr.2005.09.001
- Salthouse Timothy A., & Pink JE (2008). Why is working memory related to fluid intelligence? *Psychonomic Bulletin & Review*, 15(2), 364–371. [PubMed: 18488653]
- Santaracchi Emiliano, Polizzotto NR, Godone M, Giovannelli F, Feurra M, Matzen L, Rossi A, & Rossi S. (2013). Frequency-Dependent Enhancement of Fluid Intelligence

Induced by Transcranial Oscillatory Potentials. *Current Biology*, 23(15), 1449–1453. 10.1016/j.cub.2013.06.022 [PubMed: 23891115]

- Santarnecchi Emiliano, Brem A-K, Levenbaum E, Thompson T, Kadosh RC, & Pascual-Leone A. (2015a). Enhancing cognition using transcranial electrical stimulation. *Current Opinion in Behavioral Sciences*, 4, 171–178. 10.1016/j.cobeha.2015.06.003
- Santarnecchi Emiliano, Rossi S, & Rossi A. (2015b). The smarter, the stronger: Intelligence level correlates with brain resilience to systematic insults. *Cortex*, 64, 293–309. 10.1016/j.cortex.2014.11.005 [PubMed: 25569764]
- Santarnecchi E, Muller T, Rossi S, Sarkar A, Polizzotto NR, Rossi A, & Kadosh RC (2016). Individual differences and specificity of prefrontal gamma frequency-tACS on fluid intelligence capabilities. *Cortex*, 75(1879–0445 (Electronic)), 33–43. 10.1016/j.cub.2013.06.022
- Santarnecchi Emiliano, Emmendorfer A, & Pascual-Leone A. (2017). Dissecting the parieto-frontal correlates of fluid intelligence: A comprehensive ALE meta-analysis study. *Intelligence*, 63, 9–28. 10.1016/j.intell.2017.04.008
- Schultz DH, & Cole MW (2016). Higher Intelligence Is Associated with Less Task-Related Brain Network Reconfiguration. *Journal of Neuroscience*, 36(33), 8551–8561. 10.1523/JNEUROSCI.0358-16.2016 [PubMed: 27535904]
- Seeley WW, Menon V, Schatzberg AF, Keller J, Glover GH, Kenna H, Reiss AL, & Greicius MD (2007). Dissociable Intrinsic Connectivity Networks for Salience Processing and Executive Control. *Journal of Neuroscience*, 27(9), 2349–2356. 10.1523/JNEUROSCI.5587-06.2007 [PubMed: 17329432]
- Shehzad Z, Kelly AMC, Reiss PT, Gee DG, Gotimer K, Uddin LQ, Lee SH, Margulies DS, Roy AK, Biswal BB, Petkova E, Castellanos FX, & Milham MP (2009). The Resting Brain: Unconstrained yet Reliable. *Cerebral Cortex*, 19(10), 2209–2229. 10.1093/cercor/bhn256 [PubMed: 19221144]
- Shipstead Z, Harrison TL, & Engle RW (2016). Working Memory Capacity and Fluid Intelligence: Maintenance and Disengagement. *Perspectives on Psychological Science: A Journal of the Association for Psychological Science*, 11(6), 771–799. 10.1177/1745691616650647 [PubMed: 27899724]
- Shipstead Z, Redick TS, Hicks KL, & Engle RW (2012). The scope and control of attention as separate aspects of working memory. *Memory (Hove, England)*, 20(6), 608–628. 10.1080/09658211.2012.691519
- Shirer WR, Ryali S, Rykhlevskaia E, Menon V, & Greicius MD (2012). Decoding subject-driven cognitive states with whole-brain connectivity patterns. *Cerebral Cortex (New York, N.Y.: 1991)*, 22(1), 158–165. 10.1093/cercor/bhr099
- Simon HA, & Hayes JR (1976). The understanding process: Problem isomorphs. *Cognitive Psychology*, 8(2), 165–190. 10.1016/0010-0285(76)90022-0
- Smith EE, & Jonides J. (1999). Storage and Executive Processes in the Frontal Lobes. *Science*, 283(5408), 1657–1661. 10.1126/science.283.5408.1657 [PubMed: 10073923]
- Snyder HR, Miyake A, & Hankin BL (2015). Advancing understanding of executive function impairments and psychopathology: Bridging the gap between clinical and cognitive approaches. *Frontiers in Psychology*, 6. 10.3389/fpsyg.2015.00328
- Spearman C. (1927). *The Abilities Of Man*. Macmillan And Company., Limited. <http://archive.org/details/abilitiesofman031969mbp>
- Sporns O. (2014). Contributions and challenges for network models in cognitive neuroscience. *Nature Neuroscience*, 17(5), 652–660. 10.1038/nn.3690 [PubMed: 24686784]
- Spreng RN, Sepulcre J, Turner GR, Stevens WD, & Schacter DL (2012). Intrinsic Architecture Underlying the Relations among the Default, Dorsal Attention, and Frontoparietal Control Networks of the Human Brain. *Journal of Cognitive Neuroscience*, 25(1), 74–86. 10.1162/jocn\_a\_00281 [PubMed: 22905821]
- Stephenson CL, & Halpern DF (2013). Improved matrix reasoning is limited to training on tasks with a visuospatial component. *Intelligence*, 41(5), 341–357. 10.1016/j.intell.2013.05.006
- Sternberg RJ (2008). Increasing fluid intelligence is possible after all. *Proceedings of the National Academy of Sciences of the United States of America*, 105(19), 6791–6792. 10.1073/pnas.0803396105 [PubMed: 18474863]

- Studer BE, Jaeggi SM, Buschkuohl M, Su Y-F, Jonides J, & Perrig WJ (2009). Improving Fluid Intelligence—Single N-back Is As Effective As Dual N-back. 50th Annual Meeting of the Psychonomic Society, Boston, MA.
- Sylvester C-YC, Wager TD, Lacey SC, Hernandez L, Nichols TE, Smith EE, & Jonides J. (2003). Switching attention and resolving interference: fMRI measures of executive functions. *Neuropsychologia*, 41(3), 357–370. [PubMed: 12457760]
- Tatti E, Rossi S, Innocenti I, Rossi A, & Santarneccchi E. (2016). Non-invasive brain stimulation of the aging brain: State of the art and future perspectives. *Ageing Research Reviews*, 29, 66–89. 10.1016/j.arr.2016.05.006 [PubMed: 27221544]
- Tavor I, Parker JO, Mars RB, Smith SM, Behrens TE, & Jbabdi S. (2016). Task-free MRI predicts individual differences in brain activity during task performance. *Science*, 352(6282), 216–220. 10.1126/science.aad8127 [PubMed: 27124457]
- te Nijenhuis J, van Vianen AEM, & van der Flier H. (2007). Score gains on g-loaded tests: No g. *Intelligence*, 35(3), 283–300. 10.1016/j.intell.2006.07.006
- Thompson TW, Waskom ML, Garel K-LA, Cardenas-Iniguez C, Reynolds GO, Winter R, Chang P, Pollard K, Lala N, Alvarez GA, & Gabrieli JDE (2013). Failure of working memory training to enhance cognition or intelligence. *PLoS One*, 8(5), e63614. 10.1371/journal.pone.0063614
- Tsukiura T, Fujii T, Takahashi T, Xiao R, Inase M, Iijima T, Yamadori A, & Okuda J. (2001). Neuroanatomical discrimination between manipulating and maintaining processes involved in verbal working memory; a functional MRI study. *Cognitive Brain Research*, 11(1), 13–21. 10.1016/S0926-6410(00)00059-8 [PubMed: 11240107]
- Turkeltaub PE, Eickhoff SB, Laird AR, Fox M, Wiener M, & Fox P. (2012). Minimizing within-experiment and within-group effects in Activation Likelihood Estimation meta-analyses. *Hum. Brain Mapp*, 33(1097–0193 (Electronic)), 1–13. 10.1002/hbm.21186
- Uddin LQ, Supekar KS, Ryali S, & Menon V. (2011). Dynamic Reconfiguration of Structural and Functional Connectivity Across Core Neurocognitive Brain Networks with Development. *Journal of Neuroscience*, 31(50), 18578–18589. 10.1523/JNEUROSCI.4465-11.2011 [PubMed: 22171056]
- van der Sluis S, de Jong PF, & van der Leij A. (2007). Executive functioning in children, and its relations with reasoning, reading, and arithmetic. *Intelligence*, 35(5), 427–449. 10.1016/j.intell.2006.09.001
- Van Dijk KRA, Hedden T, Venkataraman A, Evans KC, Lazar SW, & Buckner RL (2009). Intrinsic Functional Connectivity As a Tool For Human Connectomics: Theory, Properties, and Optimization. *Journal of Neurophysiology*, 103(1), 297–321. 10.1152/jn.00783.2009 [PubMed: 19889849]
- Wang L, Song M, Jiang T, Zhang Y, & Yu C. (2011). Regional homogeneity of the resting-state brain activity correlates with individual intelligence. *Neuroscience Letters*, 488(3), 275–278. 10.1016/j.neulet.2010.11.046 [PubMed: 21108990]
- Warren DE, Power JD, Bruss J, Denburg NL, Waldron EJ, Sun H, Petersen SE, & Tranel D. (2014). Network measures predict neuropsychological outcome after brain injury. *Proceedings of the National Academy of Sciences*, 111(39), 14247–14252. 10.1073/pnas.1322173111
- Watkins MW, Lei P-W, & Canivez GL (2007). Psychometric intelligence and achievement: A cross-lagged panel analysis. *Intelligence*, 35(1), 59–68. 10.1016/j.intell.2006.04.005
- Woolgar A, Parr A, Cusack R, Thompson R, Nimmo-Smith I, Torralva T, Roca M, Antoun N, Manes F, & Duncan J. (2010). Fluid intelligence loss linked to restricted regions of damage within frontal and parietal cortex. *Proceedings of the National Academy of Sciences of the United States of America*, 107(33), 14899–14902. 10.1073/pnas.1007928107 [PubMed: 20679241]
- Yoo S-S, Paralkar G, & Panych LP (2004). Neural Substrates Associated With The Concurrent Performance Of Dual Working Memory Tasks. *International Journal of Neuroscience*, 114(6), 613–631. 10.1080/00207450490430561
- Zhao X, Wang Y, Liu D, & Zhou R. (2011). Effect of updating training on fluid intelligence in children. *Chinese Science Bulletin*, 56(21), 2202–2205. 10.1007/s11434-011-4553-5

Zuo N, Yang Z, Liu Y, Li J, & Jiang T. (2018). Core networks and their reconfiguration patterns across cognitive loads. *Human Brain Mapping*, 39(9), 3546–3557. 10.1002/hbm.24193 [PubMed: 29676536]

Author Manuscript

Author Manuscript

Author Manuscript

Author Manuscript



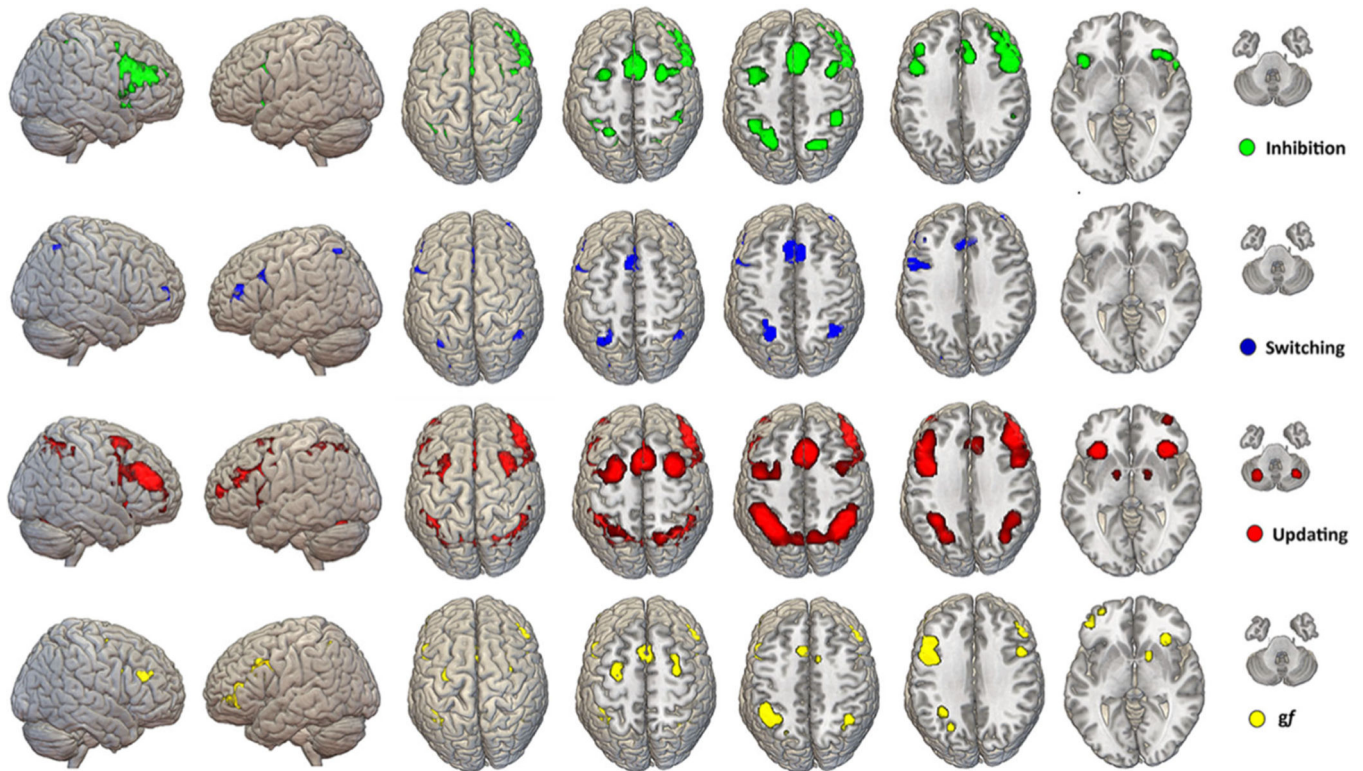


**Fig. 1.**

ALE maps. Results of the quantitative analysis of fMRI activation for *gf* and EFs tasks are shown on a template brain in MNI space. The maps are the results of voxel-wise analysis based on  $p < 0.001$  threshold for cluster-formation and a  $p < 0.05$  for cluster-level inference. On average, clusters had a dimension between 500–1,000 mm<sup>3</sup>. Amore comprehensive depiction of each EF map is available as part of the supplementary materials of the manuscript (Figures S1-2-3; Tables S2-3-4). Note: MNI = Montreal Neurologic Institute

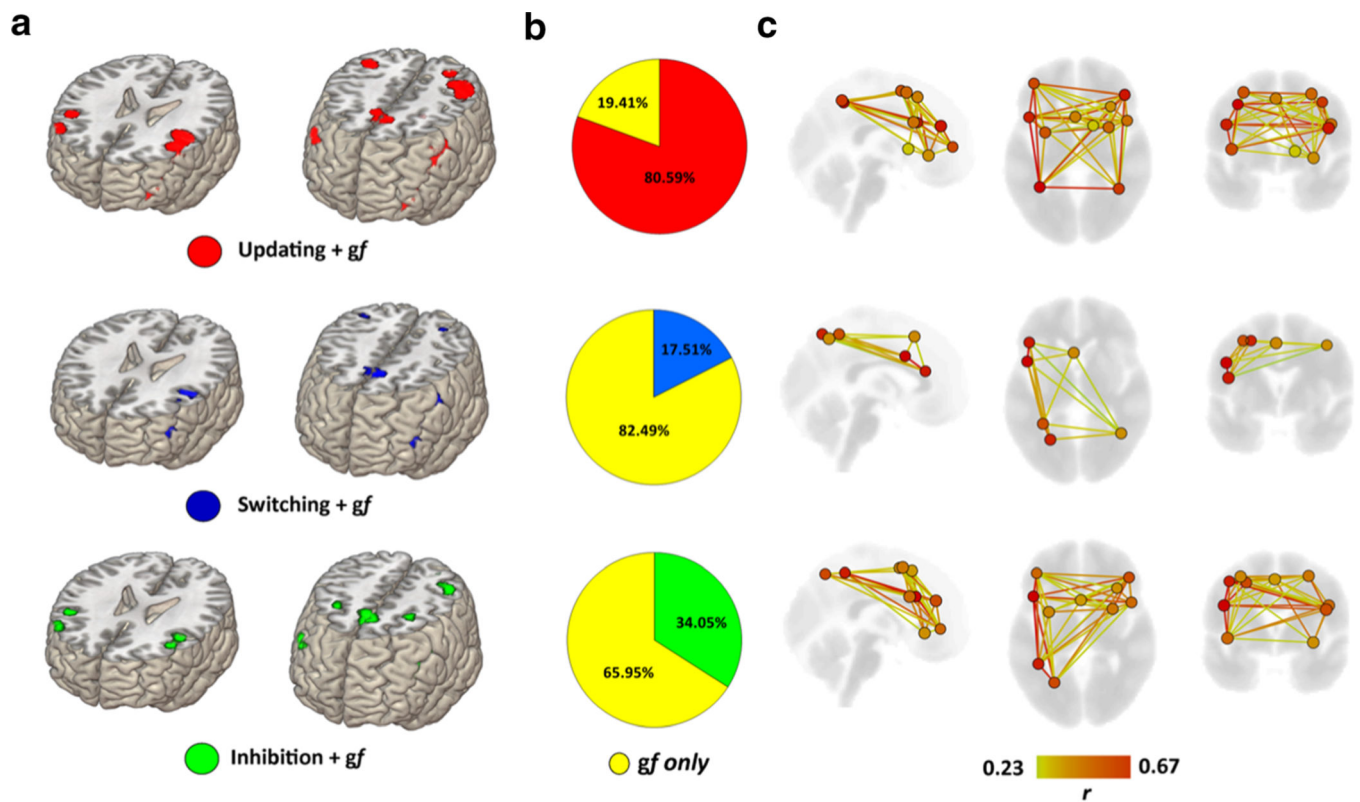


**Fig. 2.**

Statistical overlap between EFs and *gf*. Brain regions displaying statistically significant overlap between *gf* and each EFs are displayed (A), as well as the percentage of overlap of each EFs with the *gf*ALE map (B). A greater overlap between updating and *gf* was present, with the two networks showing strong overlap especially in bilateral frontoparietal regions (C). Overlapping regions are displayed as nodes of a network; their corresponding spontaneous functional connectivity pattern (Pearson  $r$  coefficient) also is shown, highlighting stronger and weaker connections within the overlapping nodes.

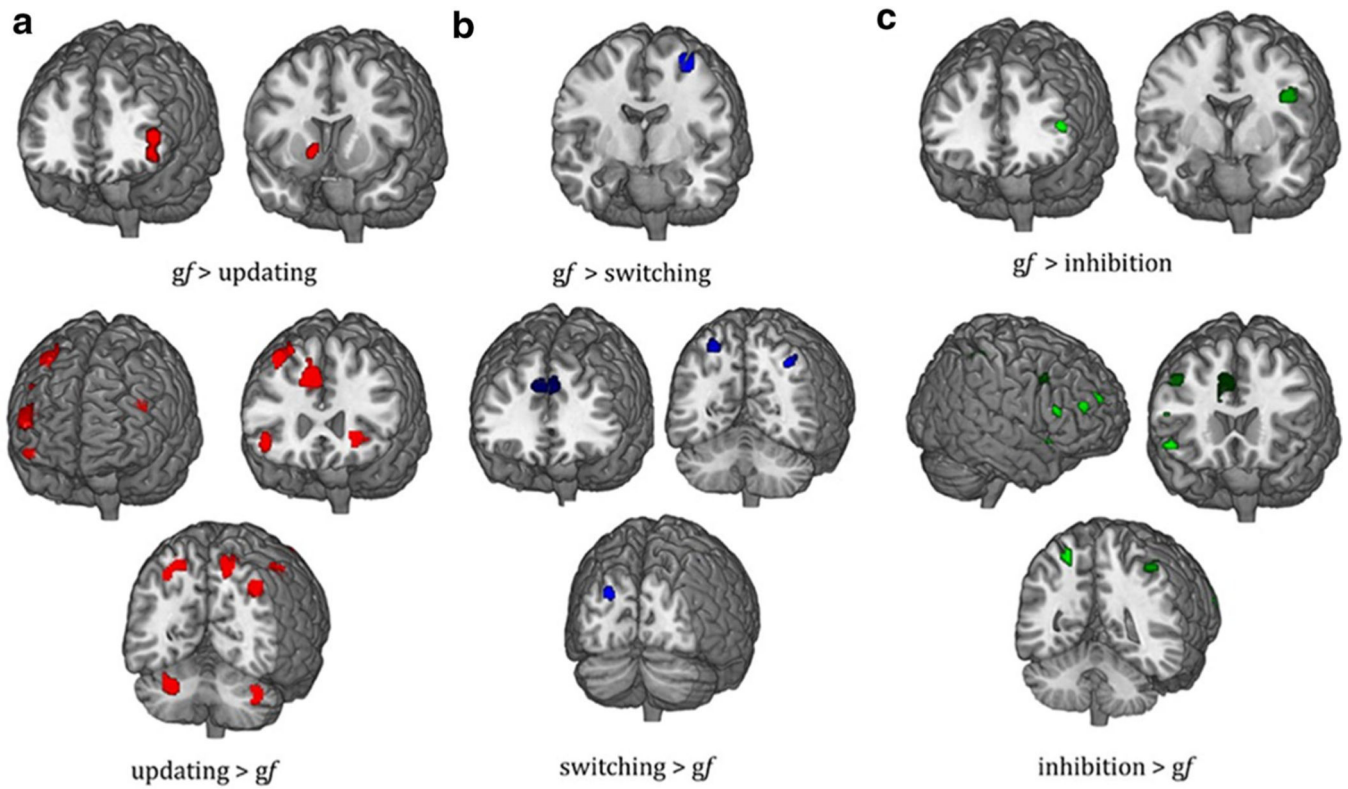


**Fig. 3.** Disjunction maps for EFs and *gf*. Significant differences in brain activation for updating and *gf* (**A**), switching and *gf* (**B**), inhibition and *gf* (**C**) are reported.

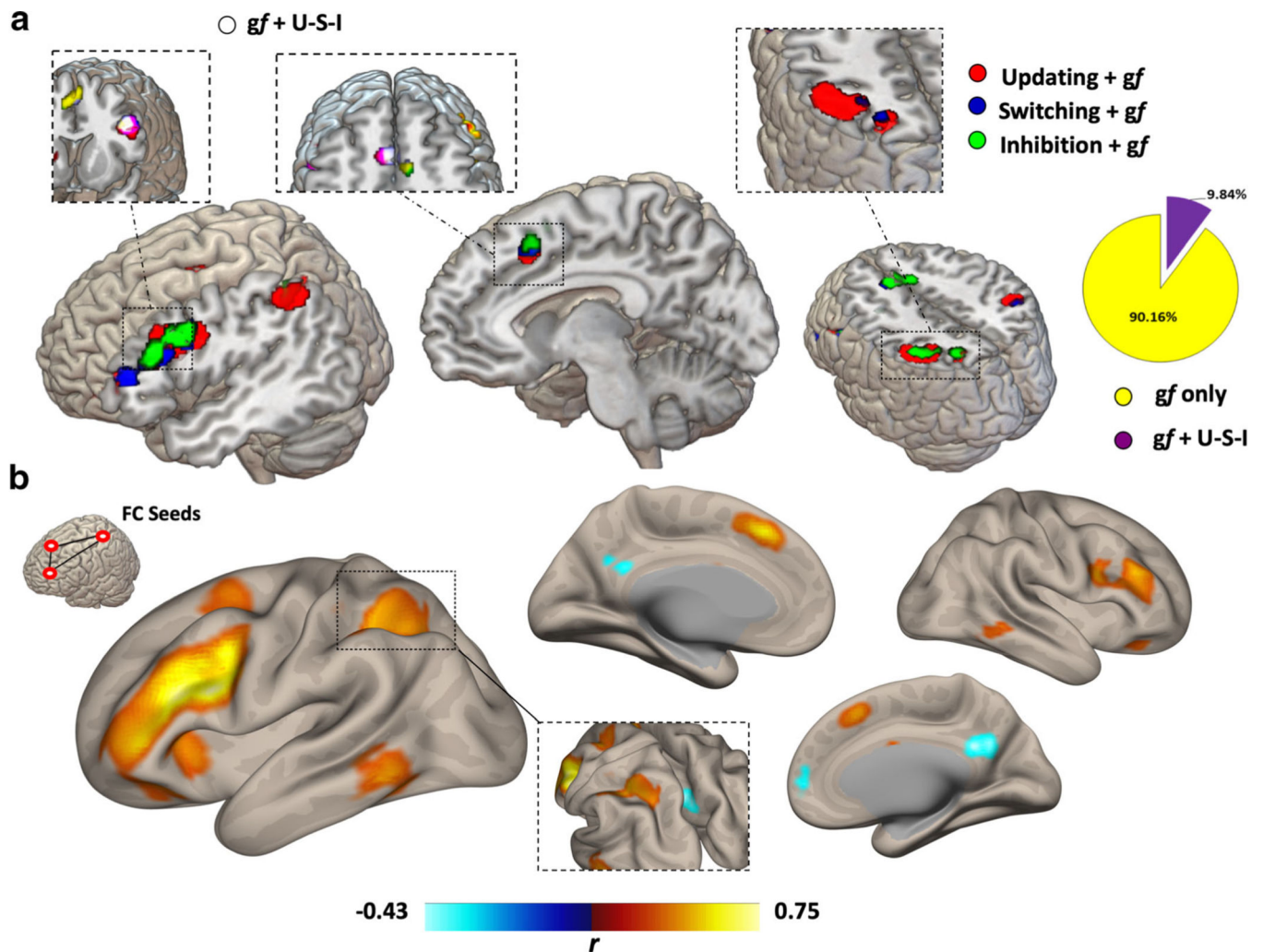


**Fig. 4.** Full overlap between EFs and *gf*. A subset of brain regions composing each EFs and *gf* maps displayed full overlap across the four functions, even though only composing roughly 10% of the *gf* map (A). The regions included the ACC, left MFG, and left IPL, with the higher overlap displayed by the left MFG as also highlighted by looking at the functional connectivity profile of the three overlapping regions (B)

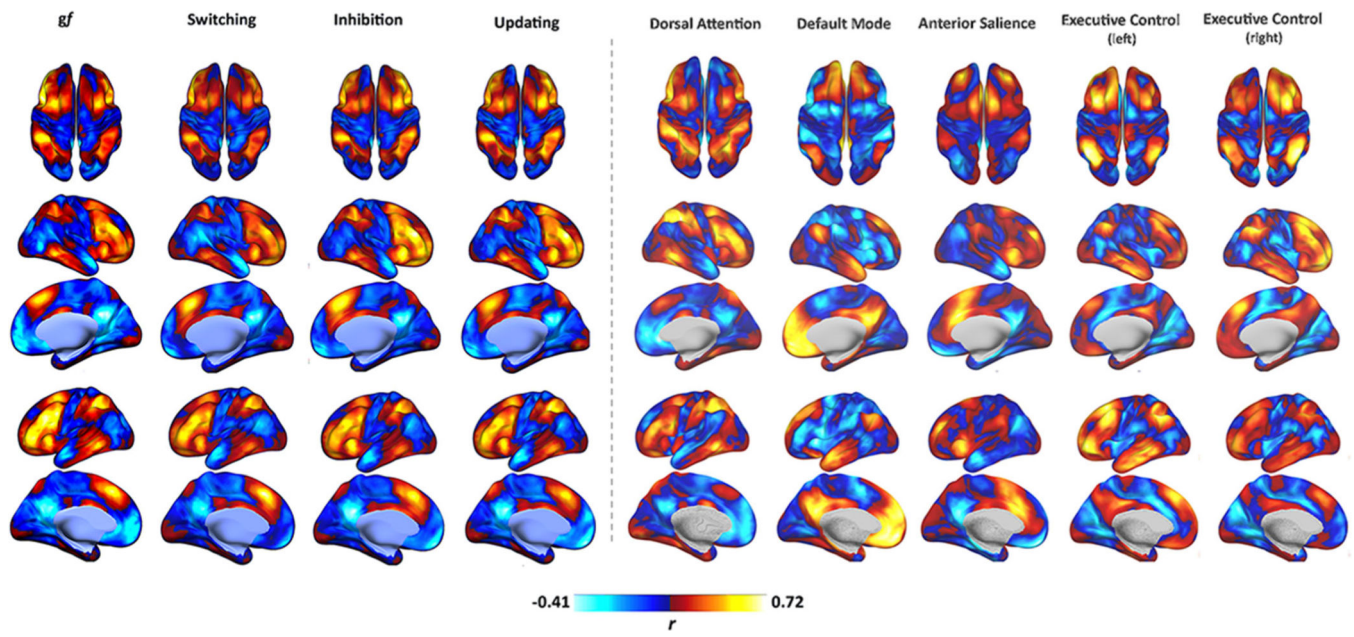


**Fig. 5.** Functional connectivity profile. As visible, *gf* and EFs maps display high similarity in terms of their functional connectivity fMRI profile, with a strong positive connectivity between their nodes and a negative connectivity with brain regions resembling the DMN. Their overall pattern also seems to resemble those of other “cognitive” RSNs, such as the FPCN and DAN. Connectivity is expressed as correlation coefficient between the average BOLD signal extracted from each map and that of any other voxel in the brain. Data refer to the FAST dataset. DMN = Default Mode Network.

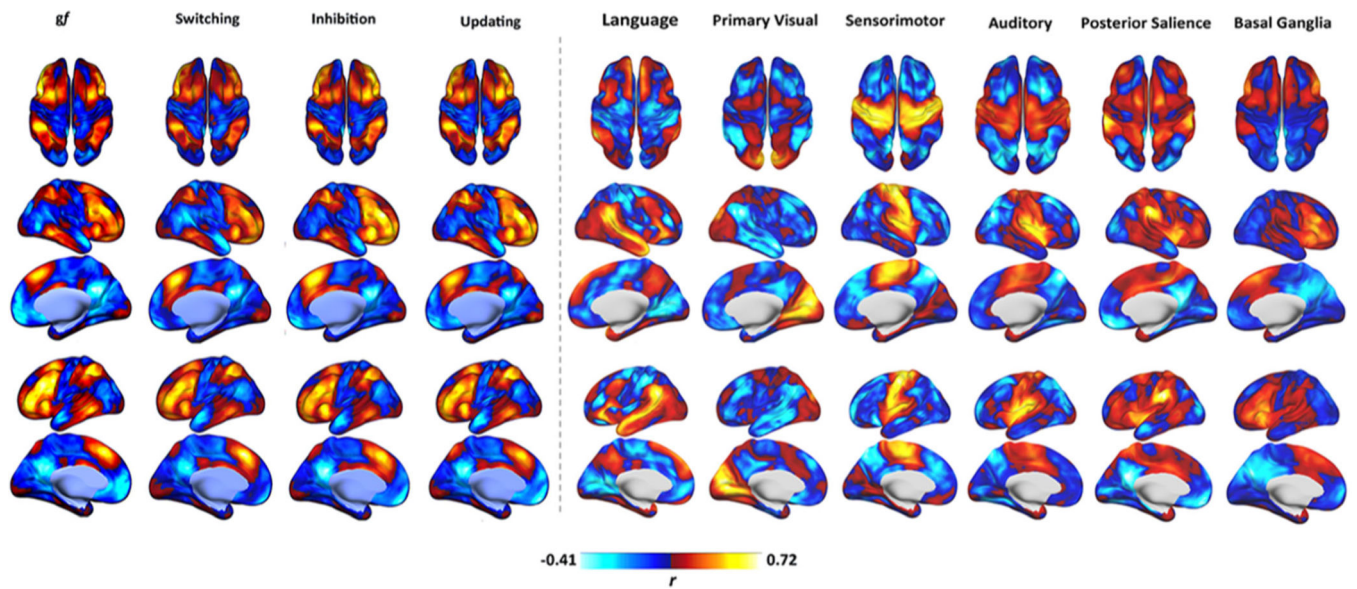


**Fig. 6.**

Functional connectivity profile of other RSNs. Gf and EFs maps display lower similarity with other RSNs, such as the visual, auditory, language, and motor networks. Connectivity is expressed as correlation coefficient between the average BOLD signal extracted from each map and that of any other voxel in the brain. Data refer to the FAST dataset. DMN = Default Mode Network.

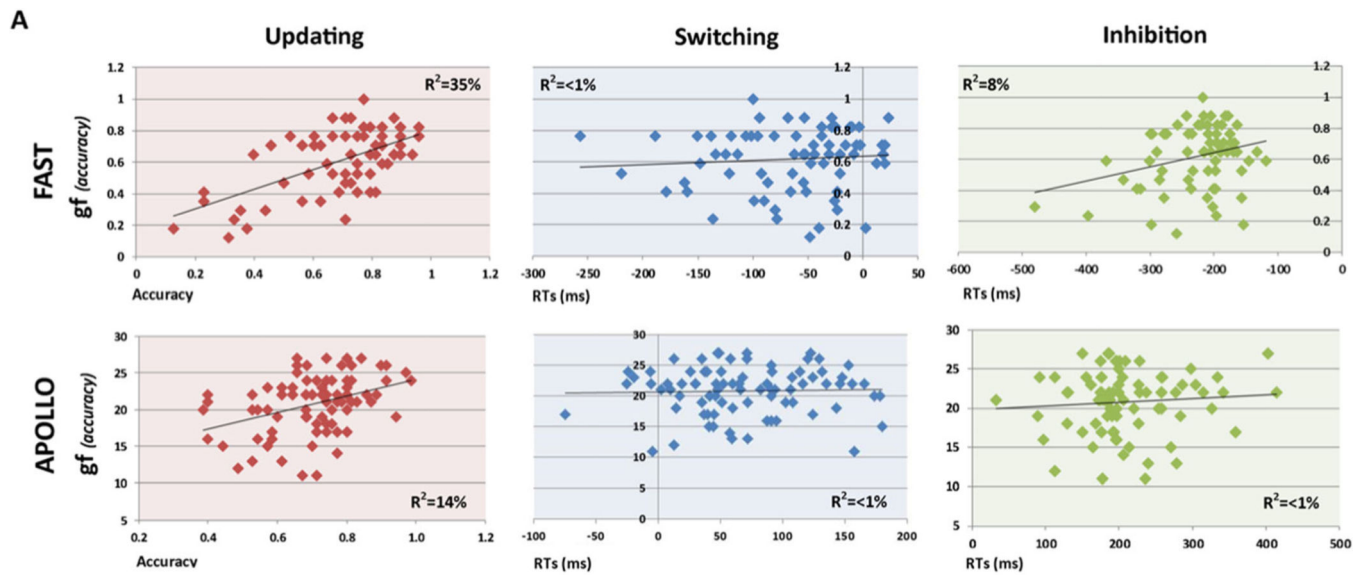


**Fig. 7.**

Behavioral correlation. As previously reported,  $g_f$  scores in both the FAST (**A**) and APOLLO (**B**) datasets display a positive correlation with updating scores, while no significant correlation is present with switching and inhibition scores in both datasets.

Table 1

Updating and *gf*: Conjunction and disjunction activation pattern for updating and *gf*

| Cluster number                 | Volume (mm <sup>3</sup> ) | GyrusWeighted Center |       |      | Extrema Value |       |     | Extrema value coordinates |    |   | Brodman Area | Hemisphere | Lobe                             | Label |
|--------------------------------|---------------------------|----------------------|-------|------|---------------|-------|-----|---------------------------|----|---|--------------|------------|----------------------------------|-------|
|                                |                           | x                    | y     | z    | x             | y     | z   | x                         | y  | z |              |            |                                  |       |
| <i>conjunction coordinates</i> |                           |                      |       |      |               |       |     |                           |    |   |              |            |                                  |       |
| 1                              | 6608                      | -47.2                | 16    | 27.1 | 0.045         | -48   | 8   | 30                        | 9  |   | L            | Frontal    | Frontal Gyrus                    |       |
|                                |                           |                      |       |      | 0.034         | -46   | 24  | 22                        | 46 |   | L            | Frontal    | Middle Frontal Gyrus             |       |
| 2                              | 5544                      | -37.8                | -49.9 | 45.9 | 0.034         | -46   | -44 | 48                        | 40 |   | L            | Parietal   | Inferior Parietal Lobule         |       |
|                                |                           |                      |       |      | 0.029         | -36   | -48 | 42                        | 40 |   | L            | Parietal   | Inferior Parietal Lobule         |       |
|                                |                           |                      |       |      | 0.026         | -24   | -64 | 44                        | 7  |   | L            | Parietal   | Precuneus                        |       |
| 3                              | 2928                      | -1.2                 | 15.1  | 49.9 | 0.025         | -4    | 18  | 48                        | 6  |   | L            | Frontal    | Superior Frontal Gyrus           |       |
|                                |                           |                      |       |      | 0.021         | 4     | 10  | 50                        | 6  |   | R            | Frontal    | Superior Frontal Gyrus           |       |
|                                |                           |                      |       |      | 0.021         | 8     | 10  | 48                        | 24 |   | R            | Limbic     | Cingulate Gyrus                  |       |
| 4                              | 1088                      | 39.1                 | -53.1 | 47.5 | 0.027         | 40    | -52 | 48                        | 40 |   | R            | Parietal   | ParietalInferior Parietal Lobule |       |
|                                |                           |                      |       |      | 0.016         | 34    | -60 | 54                        | 7  |   | R            | Parietal   | Superior Parietal Lobule         |       |
| 5                              | 1072                      | -30                  | -3    | 56   | 0.020         | -32   | -6  | 58                        | 6  |   | L            | Frontal    | Precentral Gyrus                 |       |
|                                |                           |                      |       |      | 0.019         | -30   | 2   | 52                        | 6  |   | L            | Frontal    | Middle Frontal Gyrus             |       |
| 6                              | 61064                     | 32.2                 | 25    | -3.7 | 0.034         | 32    | 26  | -4                        | 13 |   | R            | Sub-lobar  | Insula                           |       |
| 7                              | 784                       | 47.9                 | 11.5  | 26.9 | 0.028         | 48    | 12  | 28                        | 9  |   | R            | Frontal    | Inferior Frontal Gyrus           |       |
| 8                              | 776                       | 48.5                 | 33.7  | 25.9 | 0.026         | 52    | 32  | 28                        | 9  |   | R            | Frontal    | Middle Frontal Gyrus             |       |
|                                |                           |                      |       |      | 0.017         | 44    | 42  | 30                        | 9  |   | R            | Frontal    | Middle Frontal Gyrus             |       |
| 9                              | 536                       | 30.2                 | 4.7   | 54.1 | 0.020         | 30    | -2  | 56                        | 6  |   | R            | Frontal    | Middle Frontal Gyrus             |       |
|                                |                           |                      |       |      | 0.019         | 30    | 10  | 52                        | 6  |   | R            | Frontal    | Sub-Gyral                        |       |
| 10                             | 408                       | -40.9                | 49.1  | 1.5  | 0.023         | -42   | 44  | 10                        | 46 |   | L            | Frontal    | Middle Frontal Gyrus             |       |
|                                |                           |                      |       |      | 0.020         | -42   | 50  | -2                        | 46 |   | L            | Frontal    | Middle Frontal Gyrus             |       |
|                                |                           |                      |       |      | 0.020         | -36   | 54  | -4                        | 10 |   | L            | Frontal    | Middle Frontal Gyrus             |       |
| 11                             | 280                       | 15.5                 | 6.8   | 2.7  | 0.023         | 16    | 8   | 2                         | .  |   | R            | Sub-lobar  | Lentiform Nucleus                |       |
| 12                             | 8                         | -36                  | 56    | -6   | 0.018         | -36   | 56  | -6                        | .  |   | L            | Frontal    | Middle Frontal Gyrus             |       |
| <i>gf&gt;updating</i>          |                           |                      |       |      |               |       |     |                           |    |   |              |            |                                  |       |
| 1                              | 1504                      | -46                  | 42.4  | .5   | 38.905.919    | -47.3 | 43  | -2.9                      | 46 |   | L            | Frontal    | Inferior Frontal Gyrus           |       |
| 2                              | 200                       | 13.4                 | 9.9   | -2.8 | 2.820.158     | 14    | 10  | -4                        | .  |   | R            | Sub-lobar  | Caudate                          |       |



| Cluster number        | Volume (mm <sup>3</sup> ) | Gyrus/Weighted Center |       |       | Extrema Value | Extrema value coordinates |       |       | Brodmann Area | Hemisphere | Lobe       | Label                    |
|-----------------------|---------------------------|-----------------------|-------|-------|---------------|---------------------------|-------|-------|---------------|------------|------------|--------------------------|
|                       |                           | x                     | y     | z     |               | x                         | y     | z     |               |            |            |                          |
| <i>updating&gt;ef</i> |                           |                       |       |       |               |                           |       |       |               |            |            |                          |
| 1                     | 3408                      | 41.2                  | 43.7  | 20.7  | 38,905.919    | 44.2                      | 48.7  | 17.4  | 10            | R          | Frontal    | Middle Frontal Gyrus     |
| 2                     | 1992                      | -31.9                 | -65.2 | -27.8 | 38,905.919    | -32.1                     | -65.3 | -25.7 | .             | L          | Cerebellum | Uvula                    |
| 3                     | 1616                      | 31                    | 14.6  | 57.2  | 38,905.919    | 31.2                      | 17.2  | 59.2  | 6             | R          | Frontal    | Middle Frontal Gyrus     |
| 4                     | 1512                      | 8                     | 19.3  | 40.9  | 38,905.919    | 10                        | 20    | 40    | 6             | R          | Frontal    | Middle Frontal Gyrus     |
|                       |                           |                       |       |       | 37,190.166    | 6                         | 18    | 40    | 32            | R          | Limbic     | Cingulate Gyrus          |
|                       |                           |                       |       |       | 3,540.084     | 11                        | 18    | 40    | 32            | R          | Limbic     | Cingulate Gyrus          |
|                       |                           |                       |       |       | 24,521.637    | 12                        | 18    | 54    | 6             | R          | Frontal    | Superior Frontal Gyrus   |
| 5                     | 1424                      | 42.5                  | 22.7  | -8.3  | 38,905.919    | 45.7                      | 20.7  | -8.2  | 47            | R          | Frontal    | Inferior Frontal Gyrus   |
|                       |                           |                       |       |       | 37,190.166    | 46                        | 28    | -10   | 47            | R          | Frontal    | Inferior Frontal Gyrus   |
| 6                     | 1208                      | 44.4                  | -44.5 | 49.7  | 3,540.084     | 48                        | -42   | 56    | 40            | R          | Parietal   | Inferior Parietal Lobule |
|                       |                           |                       |       |       | 2,820.158     | 44                        | -46   | 46    | 40            | R          | Parietal   | Inferior Parietal Lobule |
| 7                     | 1072                      | 35.6                  | -62.1 | 43.4  | 3,540.084     | 36                        | -62   | 42    | 39            | R          | Parietal   | Angular Gyrus            |
| 8                     | 848                       | -26                   | -57.4 | 54.5  | 32,905.266    | -20                       | -58   | 56    | 7             | L          | Parietal   | Precuneus                |
|                       |                           |                       |       |       | 29,112.377    | -30                       | -58   | 48    | 7             | L          | Parietal   | Superior Parietal Lobule |
| 9                     | 760                       | 15.6                  | -62.4 | 58.4  | 37,190.166    | 18                        | -60   | 61    | 7             | R          | Parietal   | Superior Parietal Lobule |
|                       |                           |                       |       |       | 34,316.144    | 16                        | -60   | 56    | 7             | R          | Parietal   | Precuneus                |
| 10                    | 704                       | -40                   | 39.8  | 25.4  | 34,316.144    | -38                       | 44    | 25    | 9             | L          | Frontal    | Superior Frontal Gyrus   |
|                       |                           |                       |       |       | 31,213.892    | -36                       | 40    | 24    | 9             | L          | Frontal    | Middle Frontal Gyrus     |
| 11                    | 624                       | 38.6                  | -65.6 | -32.8 | 32,388.802    | 40                        | -70   | -34   | .             | R          | Cerebellum | Cerebellar Tonsil        |
| 12                    | 400                       | -44.4                 | 12.1  | 13.9  | 29,112.377    | -44                       | 12    | 12    | 13            | L          | Sub-lobar  | Insula                   |
| 13                    | 368                       | -28.1                 | 25.1  | -3.3  | 2,820.158     | -26                       | 26    | -4    | .             | L          | Sub-lobar  | Clastrum                 |
| 14                    | 328                       | 7.7                   | 35.1  | 29    | 29,888.823    | 10                        | 38    | 30    | 9             | R          | Frontal    | Medial Frontal Gyrus     |
| 15                    | 248                       | 48.7                  | 16.6  | 13    | 29,290.497    | 48                        | 16    | 12    | 13            | R          | Sub-lobar  | Insula                   |
| 16                    | 208                       | 39.6                  | 57.2  | -9    | 30,114.539    | 40                        | 60    | -12   | 10            | R          | Frontal    | Medial Frontal Gyrus     |

Table 2

Switching and gf: Conjunction and disjunction activation foci for flexibility and gf

| Cluster number                 | Volume (mm <sup>3</sup> ) | GyrusWeighted Center |       |      | Extrema Value | Extrema value coordinates |       |      | Brodman Area | Hemisphere | Lobe      | Label                    |
|--------------------------------|---------------------------|----------------------|-------|------|---------------|---------------------------|-------|------|--------------|------------|-----------|--------------------------|
|                                |                           | x                    | y     | z    |               | x                         | y     | z    |              |            |           |                          |
| <i>conjunction coordinates</i> |                           |                      |       |      |               |                           |       |      |              |            |           |                          |
| 1                              | 1592                      | -45.6                | 30.9  | 15.8 | 0.024         | -44                       | 28    | 18   | 46           | L          | Frontal   | Middle Frontal Gyrus     |
|                                |                           |                      |       |      | 0.024         | -46                       | 22    | 18   | 46           | L          | Frontal   | Middle Frontal Gyrus     |
|                                |                           |                      |       |      | 0.023         | -46                       | 40    | 10   | 46           | L          | Frontal   | Middle Frontal Gyrus     |
| 2                              | 1352                      | -49.6                | 10.6  | 30.8 | 0.026         | -52                       | 10    | 34   | 9            | L          | Frontal   | Middle Frontal Gyrus     |
|                                |                           |                      |       |      | 0.019         | -46                       | 10    | 26   | 9            | L          | Frontal   | Inferior Frontal Gyrus   |
| 3                              | 1328                      | -2.6                 | 17.9  | 47.9 | 0.025         | -4                        | 18    | 48   | 6            | L          | Frontal   | Superior Frontal Gyrus   |
| 4                              | 200                       | 39                   | -54.9 | 49.2 | 0.021         | 40                        | -54   | 50   | 7            | R          | Parietal  | Inferior Parietal Lobule |
| 5                              | 48                        | -31.3                | -50.3 | 50.6 | 0.017         | -32                       | -50   | 50   | 40           | L          | Parietal  | Inferior Parietal Lobule |
| 6                              | 40                        | -25.6                | -61.2 | 48   | 0.018         | -26                       | -62   | 48   | 7            | L          | Parietal  | Superior Frontal Gyrus   |
| 7                              | 16                        | -25                  | -64   | 50   | 0.015         | -26                       | -64   | 50   | 7            | L          | Parietal  | Superior Frontal Gyrus   |
| 8                              | 8                         | 42                   | -58   | 46   | 0.014         | 42                        | -58   | 46   | 39           | R          | Parietal  | Inferior Parietal Lobule |
| <i>gf&gt;switching</i>         |                           |                      |       |      |               |                           |       |      |              |            |           |                          |
| 1                              | 696                       | -32.3                | -4.3  | 58.5 | 29.112.377    | -34                       | -2    | 58   | 6            | L          | Frontal   | Precentral Gyrus         |
| <i>switching&gt;gf</i>         |                           |                      |       |      |               |                           |       |      |              |            |           |                          |
| 1                              | 1904                      | -2.2                 | 31.8  | 34   | 38.905.919    | -6                        | 36    | 34   | 6            | L          | Frontal   | Medial Frontal Gyrus     |
|                                |                           |                      |       |      | 37.190.166    | 6                         | 36    | 30   | 6            | R          | Frontal   | Medial Frontal Gyrus     |
|                                |                           |                      |       |      | 34.316.144    | -8                        | 30    | 28   | 32           | L          | Limbic    | Cingulate Gyrus          |
|                                |                           |                      |       |      | 3.352.795     | -8                        | 26    | 31   | 32           | L          | Frontal   | Cingulate Gyrus          |
| 2                              | 888                       | -25.8                | -57.7 | 55.1 | 34.316.144    | -21.3                     | -58.7 | 54.7 | 7            | L          | Parietal  | Superior Parietal Lobule |
|                                |                           |                      |       |      | 3.352.795     | -26                       | -60   | 56   | 7            | L          | Parietal  | Superior Parietal Lobule |
| 3                              | 448                       | 34.8                 | 53.7  | 7.1  | 34.316.144    | 32                        | 50    | 10   | 10           | R          | Frontal   | Superior Frontal Gyrus   |
|                                |                           |                      |       |      | 27.163.806    | 34                        | 58    | 2    | 10           | R          | Frontal   | Middle Frontal Gyrus     |
|                                |                           |                      |       |      | 26.437.218    | 38                        | 58    | 4    | 10           | R          | Frontal   | Middle Frontal Gyrus     |
| 4                              | 416                       | -21.1                | -84.4 | 26.3 | 2.833.787     | -20                       | -86   | 22   | 18           | L          | Occipital | Occipital Gyrus          |
|                                |                           |                      |       |      | 26.968.443    | -20                       | -80   | 26   | 18           | L          | Occipital | Cuneus                   |
| 5                              | 216                       | 37.7                 | -62.5 | 45.3 | 26.968.443    | 40                        | -64   | 45   | 19           | R          | Parietal  | Precuneus                |

Volume, coordinates, and corresponding Brodmann area, lobe, hemisphere, and regional labels are reported for each cluster of contrasts between flexibility and *g*.

Author Manuscript

Author Manuscript

Author Manuscript

Author Manuscript

Table 3

Inhibition and gf. Conjunction and disjunction activation pattern for inhibition and gf

| Cluster number                 | Volume (mm <sup>3</sup> ) | GyrusWeighted Center |       |          | Extrema Value | Extrema value coordinates |      |      | Brodmann Area | Hemisphere | Lobe      | Label                    |
|--------------------------------|---------------------------|----------------------|-------|----------|---------------|---------------------------|------|------|---------------|------------|-----------|--------------------------|
|                                |                           | x                    | y     | z        |               | x                         | y    | z    |               |            |           |                          |
| <i>conjunction coordinates</i> |                           |                      |       |          |               |                           |      |      |               |            |           |                          |
| 1                              | 12672                     | -2                   | 14.6  | 50.4     | 0.025         | -4                        | 18   | 48   | 6             | L          | Frontal   | Superior Frontal Gyrus   |
|                                |                           |                      |       |          | 0.021         | 4                         | 10   | 50   | 6             | R          | Frontal   | Superior Frontal Gyrus   |
|                                |                           |                      |       |          | 0.021         | 8                         | 10   | 48   | 24            | R          | Limbic    | Cingulate Gyrus          |
| 2                              | 2344                      | -46                  | 18.4  | 27.3     | 0.037         | -46                       | 10   | 32   | 9             | L          | Frontal   | Inferior Frontal Gyrus   |
|                                |                           |                      |       |          | 0.032         | -46                       | 26   | 22   | 46            | L          | Frontal   | Middle Frontal Gyrus     |
|                                |                           |                      |       |          | 0.025         | -48                       | 20   | 28   | 9             | L          | Frontal   | Middle Frontal Gyrus     |
|                                |                           |                      |       |          | 0.019         | -40                       | 26   | 32   | 9             | L          | Frontal   | Middle Frontal Gyrus     |
| 3                              | 1128                      | -41                  | -46.6 | 49.5     | 0.030         | -42                       | -48  | 50   | 40            | L          | Parietal  | Inferior Parietal Lobule |
|                                |                           |                      |       |          | 0.029         | -44                       | -44  | 50   | 40            | L          | Parietal  | Inferior Parietal Lobule |
| 4                              | 648                       | 48                   | 12.1  | 27.1     | 0.028         | 48                        | 12   | 28   | 9             | R          | Frontal   | Inferior Parietal Lobule |
| 5                              | 632                       | 48.3                 | 33.4  | 25.3     | 0.025         | 50                        | 32   | 26   | 9             | R          | Frontal   | Middle Frontal Gyrus     |
|                                |                           |                      |       |          | 0.017         | 44                        | 40   | 28   | 9             | R          | Frontal   | Middle Frontal Gyrus     |
| 6                              | 432                       | 29.8                 | 6.    | 53.2     | 0.019         | 30                        | -2   | 54   | 6             | R          | Frontal   | Middle Frontal Gyrus     |
|                                |                           |                      |       |          | 0.019         | 30                        | 10   | 52   | 6             | R          | Frontal   | Sub-Gyral                |
| 7                              | 384                       | -29.3                | 2.7   | 53.3     | 0.019         | -30                       | 2    | 52   | 6             | L          | Frontal   | Middle Frontal Gyrus     |
| 8                              | 296                       | -24.7                | -63.4 | 47.2     | 0.025         | -24                       | -64  | 46   | 7             | L          | Parietal  | Precuneus                |
| 9                              | 232                       | 34                   | 25.8  | -6.3     | 0.026         | 34                        | 26   | -6   | 13            | R          | Sub-lobar | Insula                   |
| 10                             | 136                       | -42                  | 38.4  | 3.8      | 0.024         | -42                       | 40   | 4    | 46            | L          | Frontal   | Inferior Frontal Gyrus   |
| 11                             | 8                         | -42                  | 40    | -2       | 0.016         | -42                       | 40   | -2   | 46            | L          | Frontal   | Inferior Frontal Gyrus   |
| <i>inhibition&gt;gf</i>        |                           |                      |       |          |               |                           |      |      |               |            |           |                          |
| 1                              | 1400                      | 7.2                  | 19.1  | 19.136.1 | 38.905.919    | 5.6                       | 16.4 | 38.8 | 24            | R          | Limbic    | Cingulate Gyrus          |
|                                |                           |                      |       |          | 37.190.166    | 9.3                       | 16.7 | 36.7 | 32            | R          | Limbic    | Cingulate Gyru           |
|                                |                           |                      |       |          | 32.388.802    | 12                        | 22   | 22   | 32            | R          | Limbic    | Cingulate Gyrus          |
|                                |                           |                      |       |          | 30.356.724    | 10                        | 28   | 22   | 24            | R          | Limbic    | Anterior Cingulate       |
| 2                              | 1184                      | 42.6                 | 13.5  | 39.8     | 38.905.919    | 40.8                      | 18.8 | 40.4 | 6             | R          | Frontal   | Middle Frontal Gyrus     |
|                                |                           |                      |       |          | 37.190.166    | 41.8                      | 10.4 | 40   | 6             | R          | Frontal   | Middle Frontal Gyrus     |

| Cluster number | Volume (mm <sup>3</sup> ) | GyrusWeighted Center |       |      | Extrema Value  | Extrema value coordinates |       |      | Brodmann Area | Hemisphere | Lobe     | Label                    |
|----------------|---------------------------|----------------------|-------|------|----------------|---------------------------|-------|------|---------------|------------|----------|--------------------------|
|                |                           | x                    | y     | z    |                | x                         | y     | z    |               |            |          |                          |
| 3              | 672                       | 43.2                 | -37.5 | 54.1 | 3.540.084      | 48                        | 14    | 40   | 8             | R          | Frontal  | Middle Frontal Gyrus     |
| 4              | 632                       | 5.6                  | 37.3  | 28.9 | 38.905.919     | 41.1                      | -36.6 | 54.6 | 40            | R          | Parietal | Inferior Parietal Lobule |
|                |                           |                      |       |      | 38.905.919     | 3.5                       | 39    | 23.5 | 32            | R          | Limbic   | Cingulate Gyrus          |
|                |                           |                      |       |      | 37.190.166     | 6                         | 40    | 28   | 9             | R          | Frontal  | Medial Frontal Gyrus     |
|                |                           |                      |       |      | 34.316.144     | 6                         | 40    | 34   | 6             | R          | Frontal  | Medial Frontal Gyrus     |
|                |                           |                      |       |      | 30.902.324     | 8                         | 38    | 38   | 8             | R          | Frontal  | Medial Frontal Gyrus     |
| 5              | 592                       | 48.5                 | 22.3  | -8.2 | 38.905.919     | 48                        | 24    | -8   | 47            | R          | Frontal  | Inferior Frontal Gyrus   |
|                |                           |                      |       |      | 3.540.084      | 48                        | 20    | -9   | 47            | R          | Frontal  | Inferior Frontal Gyrus   |
|                |                           |                      |       |      | 32.388.802     | 54                        | 14    | -10  | 22            | R          | Temporal | Superior Temporal Gyrus  |
|                |                           |                      |       |      | 29.478.426     | 54                        | 10    | -6   | 22            | R          | Temporal | Superior Temporal Gyrus  |
| 6              | 512                       | -23                  | -54.9 | 58.4 | 38.905.919     | -20.7                     | -54   | 60.7 | 7             | L          | Frontal  | Precuneus                |
| 7              | 384                       | 54.4                 | 27.4  | 14.8 | 14.837.190.166 | 56.7                      | 27.3  | 14   | 45            | L          | Frontal  | Inferior Frontal Gyrus   |
|                |                           |                      |       |      | 29.478.426     | 50                        | 22    | 14   | 46            | R          | Frontal  | Middle Frontal Gyrus     |
| 8              | 336                       | 44.6                 | 47    | 17.1 | 38.905.919     | 44                        | 50    | 17   | 10            | R          | Frontal  | Middle Frontal Gyrus     |
| 9              | 312                       | 28.3                 | 54    | 22.8 | 38.905.919     | 28.6                      | 53.5  | 23.2 | 10            | R          | Frontal  | Superior Frontal Gyrus   |
| 10             | 208                       | -37.6                | 43.1  | 20.6 | 37.190.166     | -37                       | 41    | 21   | 9             | L          | Frontal  | Middle Frontal Gyrus     |
|                |                           |                      |       |      | 32.905.266     | -38                       | 46    | 22   | 9             | L          | Frontal  | Middle Frontal Gyrus     |

Volume, coordinates, and corresponding Brodmann area, lobe, hemisphere, and regional labels are reported for each cluster included in the ALE map.